Sevenfold variation in global feeding capacity depends on diets, land use and nitrogen management

Petros Chatzimpiros, Souhil Harchaoui

Sevenfold variation in global feeding capacity depends on diets, land use and nitrogen management

Petros Chatzimpiros[1*] and Souhil Harchaoui[2*]

petros.chatzimpiros@u-paris.fr
souhil.harchaoui@inrae.fr

[1] Université Paris Cité, LIED, CNRS UMR 8236, F-75013 Paris, France
[2] INRAE, Institut Agro Rennes-Angers, UMR SAS, 35000 Rennes, France
[*] Corresponding authors

This document is a preprint of the following paper:

Chatzimpiros, P., Harchaoui, S., 2023. Sevenfold variation in global feeding capacity depends on diets, land use and nitrogen management. Nat. Food. https://doi.org/10.1038/s43016-023-00741-w

Please cite this reference if you mention this work

Harvested food carries a fraction of the nitrogen applied through fertilization; the remainder is typically lost into the environment, impairing planetary sustainability. Using a global agriculture model that integrates key drivers of food production and nitrogen cycling, we simulated upper bounds to global feeding capacity – and associated nitrogen pollution – in function of nitrogen limitation under organic and industrial fertilization regimes. We found that the current agricultural area could feed ca. 8-20 billion people under unconstrained industrial fertilization and ca. 3-14 billion under organic fertilization. These ranges are inversely correlated with animal proteins in human diets, and are a function of feed-food competition, grassland-to-cropland allocation, and – in the case of organic fertilization – nitrogen use efficiency. Improved nitrogen use efficiency is required to bring nitrogen pollution within planetary sustainability limits and is also essential in narrowing down food productivity gaps between organic and industrial fertilization regimes.

The feeding capacity of agriculture, or the supportable global population as constrained by food, depends on global agricultural area and human-edible production per hectare (the so-called 'food yield'). Today, agriculture is the largest human land appropriation on Earth, covering nearly 40% of ice-free land[1] – a tenfold increase in twenty centuries[2] – and global population is higher than ever. However, agricultural land, food yield and, thereby, agriculture's global feeding capacity, are subject to upper limits. Considering Earth system sustainability thresholds[3,4], agricultural land expansion is widely dismissed as highly unsustainable[5–9]; in the case of food yield, upper bounds echo biophysical constraints in plants and livestock, as well as factors such as global agricultural land allocation between cropland and grassland, crop mix, human diets composition and nutrients management. An integrated analysis of these factors is necessary for framing the option space of global food production.

Because proteins are essential nutrients and their production relies on reactive nitrogen (N), global food production is conditioned by N availability[10,11]. Global N availability and crop productivity have dramatically increased with the development of fossil-fueled industrial N fertilizers by the early 20th century[11], which have enabled the decoupling of global population growth from agricultural land expansion[12,13]. As a side-effect, increased N availability combined with poor N use efficiency in agriculture have triggered massive global N pollution with adverse impacts on climate, water resources, air quality, biodiversity, ecosystem services, economic development and human health[10,14,15]. By dismissing future global agricultural area expansion as unsustainable[3], upper bounds to the food yield govern the maximum edible output of global agriculture and, thereby, the upper global feeding capacity and associated N pollution.

The issue of global feeding capacity has been raised since the work of Antoni van Leeuwenhoek (1679, ref. [16]), who coined an upper estimate of 13.4 billion people on Earth by extrapolating the population density in the Netherlands at that time on the entire inhabitable surface of Earth. Much later, Thomas Malthus (ref. [17]) published his notorious prediction that human population growth would be limited by linearly growing food production, which has proven wrong to date thanks to agricultural land expansion combined with stepwise crop yield increases under abundant fertilization and mechanization[18]. By the early 21st century, over hundred estimates of maximum supportable global population had been published, diverging by more than two orders of magnitude (from about 1 to 100 billion people[16,19,20]). Despite great interest in this question and the diversity of approaches used to answer it, there is still poor understanding of the mechanisms, key drivers and constraints that shape the global feeding capacity.

Here, we develop a deterministic model – the Agricultural Limits quantification through PHysical flows Analysis in cropland, grassland and livestock compartments ('ALPHA' – see Methods and Extended Data Figure 1 for a flow diagram) – to simulate the global feeding capacity and N pollution within an option space of diets, land use and N flows management. This model accounts for total agricultural area and captures essential trade-offs that affect food productivity, diets composition and N pollution. Also, it addresses global feeding capacity and N loss in function of feed-food competition, grassland-to-cropland allocation and N management without inherent assumptions on future diets composition or implicit organic-to-industrial crop yield gaps[21,22]. Food productivity was simulated as a function of six drivers that are commonly documented in reference databases, and that we integrated with a dozen drivers of agricultural N cycling including N input, use efficiency and biowaste N return from food supply to agriculture. We calibrated and validated the model with global scale data from the United Nations Food and Agricultural Organization (FAOSTAT) and existing literature over the benchmark period 1961-2013 following a three-step process. First, we calibrated model input variables with available global weighted average data. Then, in a validation step, we confirmed the modeled feeding capacity and N cycling indicators with additional published data. After validation, we recalibrated the model by setting model input drivers at literature-derived upper thresholds, and simulated five global food production boundaries, i.e. maximum feeding capacity and associated environmental N loss under industrial and organic fertilization regimes. We found the global feeding capacity – considering total present agricultural area – to be ~8-20 billion people under industrial and ~3-14 billion under organic fertilization. We outline that under organic fertilization, N limitation is critically controlled by N loss, meaning that N use efficiency is essential for helping bridge food productivity gaps between organic and industrial systems. Our population estimates intersect with current UN projections for the 21st century[23] at levels that define global food demand compatibility with global average composition of diets, cropland-to-grassland allocation and

N management. Associated with food production, we show that global N loss is ~0.5-3 times the medium threshold suggested for planetary N sustainability[24] – a threshold that has been transgressed since the early 1960s. We discuss the relative change required in key drivers of food production and N cycling to meet 21st-century global food and N sustainability challenges.

Key drivers of food yield

Food yield at the global scale (Y_{food}) corresponds to global weighted average food productivity i.e. global human-edible harvest per unit agricultural area. For the purposes of our analysis, an adequate Y_{food} means that global food production is enough for meeting global food demand (both expressed in proteins), whereas heterogeneity in respective spatial distributions is balanced through trade[25]. Accordingly, Y_{food} sets an upper bound to global feeding capacity, as it implies a perfect match in space and time between food availability and demand[26]. We modeled global weighted average Y_{food} and its content in animal proteins as a function of six drivers, four of which are positive and two of which are negative (Fig.1a and Methods). The four positive drivers, namely crop yield (Y_{crop}), grass yield (Y_{grass}), livestock nitrogen conversion efficiency (NCE) and crop residues used for feed ($\alpha_{residues}$), are subject to biophysical upper bounds. Upper bounds have been recently specified for Y_{crop} by previous studies based on biophysical factors analysis in world regions[27], and also condition crop residues production according to the harvest index of crops, i.e. the ratio of human-edible to total crop mass. Of all crop residues, $\alpha_{residues}$ is an allocation choice between food, energy, materials and soil conservation strategies[28]. Similarly, Y_{grass} is biophysically bounded (although upper bounds remain elusive due to significant heterogeneity and uncertainty in grassland areas[29,30]). For NCE, upper bounds are specific to animal products[31] – and, for this reason, largely depend on dietary preference between animal products. The two remaining drivers, namely the share of crops used for feed (α_{crops}) and the share of grassland in global agricultural area (τ), are negative since they divert primary biomass from direct human use. These two negative drivers are not biophysically constrained and vary according to dietary preferences, soil and climate conditions and ecological valuation of resources[32,30].

Based on FAOSTAT data[33], we reconstructed the six drivers of Y_{food} (Extended Data Figure 2a-f), global agricultural area (Supplementary Figure 1), total feed and livestock production (Extended Data Figure 3a,b) from 1961 to 2013, and modeled the global weighted average Y_{food} over the benchmark period. Y_{food} controls the maximum global feeding capacity depending on average food supply per capita, as well as on human edible-harvest allocation to seed, losses and other uses. Our modeled Y_{food} has tripled from 3.2 $kgN \cdot ha^{-}1 \cdot yr^{-1}$ in 1961 to 9.2 $kgN \cdot ha^{-1} \cdot yr^{-1}$ in 2013, and was validated by data reporting global weighted average human-edible harvest per capita over the period[34] (Fig.1b). Following the FAOSTAT Food Balance Sheets classification, “food supply” in Y_{food} represented 71-83% over the period, “seed” 13-5%, and “other uses and losses” 6-17% (Fig.1b and Supplementary Figure 2). Total human-edible harvest has tripled from 14 to 44 $TgN \cdot yr^{-1}$ and has increased global population by 130%, global weighted average food supply per capita by 27% (Supplementary Figure 3), animal proteins in diets (excluding seafood) by 54%, other uses by 815%, as well as losses (between harvest and the household) by 35% against a drop in seed by 52% (ref. [33]). In parallel, the share of grassland in global agricultural area (τ) has decreased from ~78% in 1961 to ~72% in 2013 (Extended Data Figure 2f), suggesting a concomitant reduction in the ecological value of global agricultural area over the last decades[32,35,36].

To stress the competing relationship between the share of animal proteins in diets and τ, we constructed in Fig.1c a theoretical trade-off curve between the two negative drivers of Y_{food} (α_{crops}

and τ) by setting the four positive drivers (Y_{crop}, Y_{grass}, NCE, $\alpha_{residues}$) at 2013 levels. The trade-off curve shows that the same Y_{food} level as in 2013 could theoretically be sustained through various combinations of α_{crops} and τ, meaning that the share of grassland could increase when animal proteins in diets decrease, and vice versa. Of course, large-scale τ change is not a pure human choice, but also depends on soil and climate conditions. Nonetheless, as a thought experiment, our trade-off curve suggests that by lowering global τ at 31%, current (2013) global population could be theoretically fed even with a generalized western diet (55% animal proteins). In this line, the ongoing westernization of diets at the global scale[37] might be a threat to global grassland as it might drive τ down as it happened since year 2000. We argue that the trade-off between α_{crops} and τ raises key dilemmas on how future increases in crop yields and other food productivity factors should be allocated among human population growth, animal proteins in diets[38] and τ increase for sustainability[10,26].

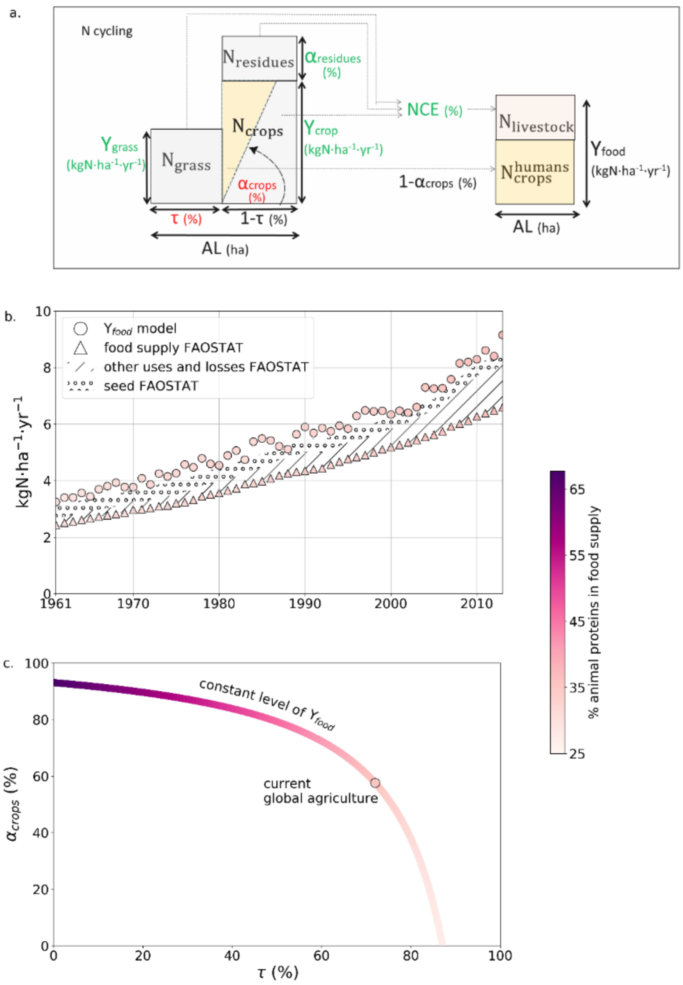

Fig. 1|Food yield modeling. a. Schematic representation of the six food yield (Y_{food}) drivers and total agricultural land (AL). The positive drivers (in green letter) are the crop yield (Y_{crop}), grass yield (Y_{grass}), share of crop residues used for feed ($\alpha_{residues}$) and livestock nitrogen conversion efficiency (NCE). The negative drivers (in red letters) are the share of crops used for feed (α_{crops}) and the share of grassland in global agricultural area (τ). Dotted arrows connect primary production from cropland (N_{crop} and $N_{residues}$) and grassland (N_{grass}) to human-edible vegetal (N^{humans}_{crops}) and animal ($N_{livestock}$) production. **b**. Global average Y_{food} simulated in function of the six drivers over the benchmark period (1961-2013) and validated upon FAOSTAT Food Balance Sheets data reporting total human-edible harvest per capita and use. The color grid displays the share of animal proteins in food supply. **c.** Theoretical trade-off curve between animal proteins in food supply (color grid), τ, and α_{crops} for a given level of Y_{food} (here 2013 level). The trade-off curve emphasizes the competing relationship between α_{crops} and τ, but does not imply that cropland-to-grassland allocation is a pure human choice.

Global food production boundaries

Global weighted average Y_{food} as defined by the six drivers is a fraction of global N input per unit agricultural area and defines total agricultural N use efficiency (NUE_{tot}); the remaining fraction is environmental N loss per unit area (r_{loss}). By connecting N input and use efficiency in cropland, grassland and livestock production to Y_{food} and r_{loss} (see Methods, Extended Data Figure 1 and Extended Data Table 1), we simulated five global food production boundaries – three under industrial (B1, B2, B3) and two under organic fertilization (B4, B5). Keeping today's total agricultural area constant (Supplementary Table 1), the five boundaries frame the global feeding capacity and N pollution by considering, on the one hand, wide ranges of feed-food competition (α_{crops} from 0 to 70%) and grassland-to-cropland allocation (τ from 72.2 to 70% i.e. 100 million hectares of grassland conversion to cropland) and, on the other hand, a variety of production practices and literature-derived upper thresholds to food productivity. The classification of model variables between input and output in each simulation and the model input data used in B1-B5 are detailed in Methods and summarized by comparison to 1961 and 2013 in Extended Data Tables 2 and 3. The model input data in B1-B5 reflect plausible global improvements based on literature estimates, past trends (Extended data Figure 2 and Supplementary Figures 1-8) and, as far as N use efficiency in cropland is concerned, best performing countries (Supplementary Figures 9-10). In B1-B3, industrial fertilization enables unconstrained N input, which – in absence of other limiting factors – supports the full closure of crop yield gaps worldwide (ref. [27] and Supplementary Table 2). In B4-B5, crop yields are a function of N limitation and are simulated across wide ranges of total biological N fixation (BNF from currently 70 to 100 TgN), biowaste N return to agriculture (from currently 5 to 30%) and improved N use efficiency. The considered increase in total BNF combines extensive integration of fodder legumes in rotations, including a full plantation of current fallow land, legume-enriched grasslands and green manures intensification in cropland. Under unconstrained fertilization, N use efficiency governs N input requirement and r_{loss}, whereas under N limitation, N use efficiency and r_{loss} govern food productivity. Across B1-B5, global average N use efficiency is set to range from levels as low as today in B1 and B4 – 44% for cropland and 35% for manure N management (Supplementary Figures 7,8) – to very ambitious levels[39,40] i.e. 70% in cropland in B2, B3 and B5 and 80% in manure N management in B3 and B5. The model was analyzed for sensitivity to input variables in Supplementary Figures 11-13.

Fig.2 shows the five global food production boundaries (B1-B5) and puts them in perspective with global weighted Y_{food} and r_{loss} as simulated over the benchmark period. Note that the maximum global feeding capacity is independent of the spatial distribution of agricultural production and demand. Indeed, weighted global average data provide sufficient information for assessing the supportable global population, while spatial heterogeneity and subsequent regional food surpluses and deficits are balanced through trade[25]. Trade is considered a "zero-sum game" at the global scale, as total imports and exports cancel out. In addition, Y_{food} and the supportable population were calculated in terms of proteins, which vary less than calories with production practices. In particular for animal products, fat tissues are easier to produce than protein tissues[41], meaning that adequate protein intake in human diets also implies sufficient calories intake.

We found that maximum feeding capacity of global agricultural area ranged from ~8 to ~20 billion people under industrial fertilization (B1-B3) and from ~3 to ~14 billion under organic fertilization (B4-B5), depending on animal proteins in diets, grassland-to-cropland allocation and N cycling. In B1-B3, τ decrease allowed for an increase of total feeding capacity thanks to unconstrained N input, whereas in B4-B5 the τ change had a limited effect due to N limitation (Extended Data Figure 4).

In all five food production boundaries, Y_{food} varied with feed-food competition (α_{crops}), while r_{loss} varied with N use efficiency (but in contrast to industrial fertilization, N use efficiency under organic fertilization also governs Y_{food}). Indeed, r_{loss} virtually equates to a negative harvest, meaning that r_{loss} abatement under N limitation is a way to close crop yield (Y_{crop}) gaps. Global average Y_{crop} ranged from 18 to 26 $kgN \cdot ha^{-1} \cdot yr^{-1}$ in B4 against 36 to 74 $kgN \cdot ha^{-1} \cdot yr^{-1}$ in B5, meaning that, by comparison to B1-B3, Y_{crop} gaps are of 65-75% in B4 against 0-51% in B5. These gaps reflect, on the one hand, differences in N input and recycling in cropland, which are function of BNF rates, ρ and α_{crops}, and, on the other hand, N use efficiency. As highlighted in Fig.2, the same increase in N input (through higher BNF and ρ) had a much more limited effect on productivity in B4 (low N use efficiency) than in B5 (high N use efficiency). We argue that one of the reasons for the disagreement in the literature on productivity gaps between industrial and organic systems is that N use efficiency is largely neglected[42,43].

Current population projections for the 21st century (ref. [23] and Supplementary Figure 14) intersect with the feeding capacity in B1-B3 and in B5, whereas B4 clearly falls below challenges due to unimproved N use efficiency. Naturally, in all cases, the feeding capacity maximizes for zero feed-food competition (α_{crops}=0), but this is not synonymous to vegan diets due to livestock production from grassland and crop residues. In B1-B3, the diet that maximizes the feeding capacity (~20 billion people) contains, on average, 15% animal proteins compared to 35% today. In B5, the global feeding capacity maximizes for ~20% animal proteins in the diet at 13.90 billion people. In B4, due to low Y_{crop}, the minimum share of animal proteins in the diet (when α_{crops} is zero) is 35%, and maximum population is 7.4 billion. Assuming vegan diets (that is, no consumption of animal proteins), the feeding capacity falls to 17.4 billion people in B1-B3 – which is 11% below the estimated maximum. Because vegan diets further imply reduced nutrient transfer from grassland to cropland, the feeding capacity in B5 falls to 6.6 billion people. N input per source over the benchmark period 1961-2013 and in B1-B5 is shown in Supplementary Figure 6 and Extended Data Figure 5, respectively.

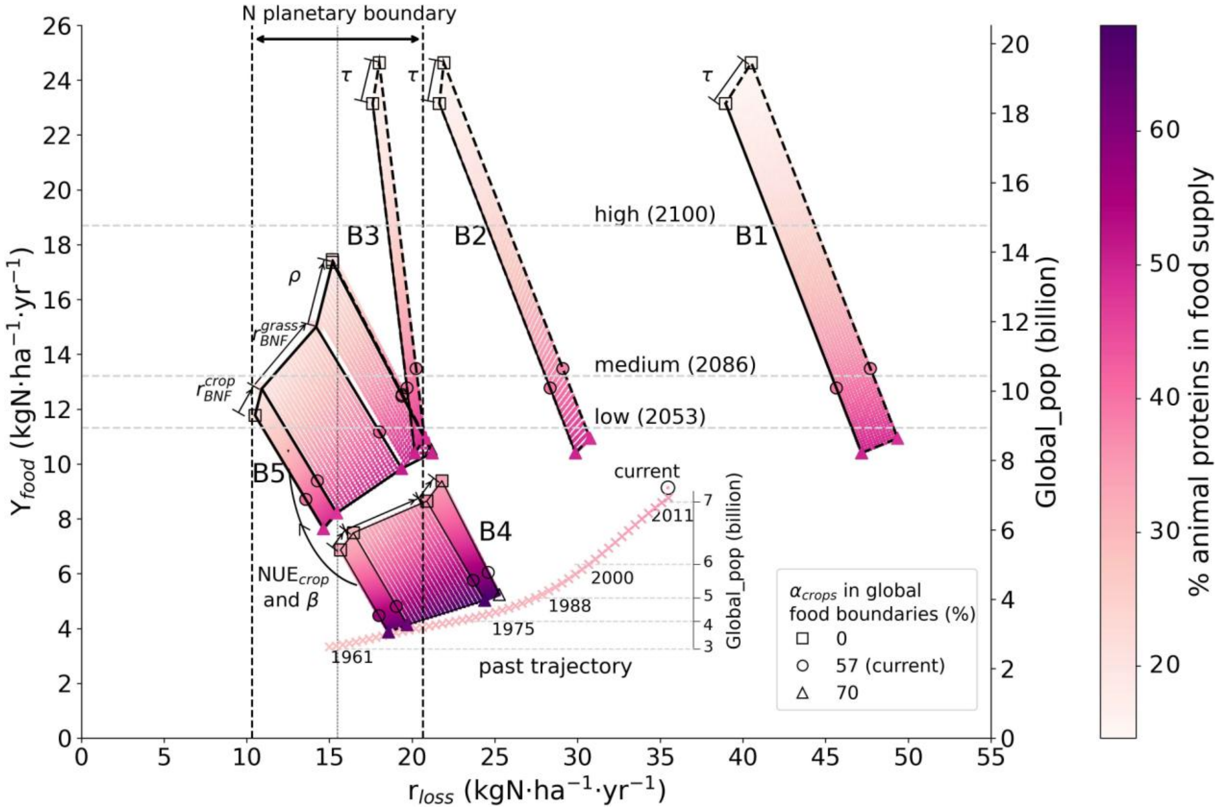

Fig.2| Food yield (Y_{food}, left axis), feeding capacity ($Global_{pop}$, right axis) and N loss rate (r_{loss}) in the five global food production boundaries (B1 to B5) and over the benchmark period (1961-2013, inset figure). B1-B3 are under industrial fertilization (full closure of crop yield gaps worldwide) and B4-B5 are under organic fertilization (crop yields depending on N limitation). The color grid displays the share of animal proteins in food supply. The feeding capacity is compared to current UN population projections (low, medium and high variants – the peak date is given in brackets). Across B1-B5, feed-food competition (α_{crops}) drives $Global_{pop}$ and r_{loss}. In B1-B3, dotted borders indicate decrease in the share of grassland (τ) in total agricultural area from 72.3 to 70.2 %. In B4-B5, borders indicate successive increases in biological N fixation rate in cropland (r_{BNF}^{crop}), grassland (r_{BNF}^{grass}) and biowaste N return to agriculture (ρ). N use efficiency in cropland (NUE_{crop}) and the share of manure N recovered to cropland (β) range from current levels in B1 and B4 to ambitious thresholds in B3 and B5. The irregular population axis in the inset figure is due to agricultural land expansion over the benchmark period paired with changing allocation of Y_{food} between food supply and other uses. The vertical dotted lines indicate the lower, medium and upper thresholds of r_{loss} proposed in the literature for planetary N sustainability.

Our results show that to reach the medium UN variant of 10.4 billion people, animal proteins in diets should not exceed ~40% in B1-B3 and ~37% in B5 (which are slightly higher levels than current global average, i.e. 35% - excluding seafood). A reduction of animal proteins in diets to 26%, as recommended in healthy diets (Supplementary Table 3) would allow feeding ~13.6 billion people in B1-B3 and ~12.2 billion in B5 – the associated livestock production is 16.3 TgN in B1-B3 and 14.8 TgN in B5 (Extended data Figure 6). In contrast, the high UN variant (14.7 billion people) is out of reach in all cases even with healthy diets, and only becomes reachable for diets containing less than 23% animal proteins. By extrapolating the current share of animal proteins in western diets (55%) at the global scale, and even after conversion of 100 Mha of grassland to cropland, the low UN variant of about 8.9 billion people is also out of reach. In B4 and B5, with current diets but without improvement in biological N fixation and biowaste N return to agriculture, the feeding capacity is about 5 and 7.5 billion people respectively. Note that crop productivity in the simulations assumes current crop mix (Supplementary Table 1) – dominated by cereals, i.e. the highest yielding crops – implying that crop mix change toward more vegetables, fruits and nuts as per health recommendations[44] might result in reduced land productivity and decreased global feeding capacity in particular in B1-B3. Similarly, increases in the share of other uses and post-harvest loss or in global average per capita food supply above 2013 levels (Supplementary Figures 2,3) would also reduce the global feeding capacity across B1-B5.

Changes in nitrogen use efficiency

Total N use efficiency (NUE_{tot}), i.e. the ratio of Y_{food} to total N input, decreased between 1961 and 1980 and increased afterwards under continuous growth in Y_{food} (Fig.3a). Currently, NUE_{tot} is ~20%, which is barely 3% higher than in the mid-1960s and ~6% higher than the observed minimum in the 1980s. Nitrogen use efficiency in cropland alone (NUE_{crop}) has decreased in time and is today 44%, which is in line with previous estimates[40,45](Supplementary Figure 8). Cropland is by far the most studied agricultural land use in the literature, but the gap between NUE_{crop} and NUE_{tot} highlights the importance of other agricultural land uses for food systems sustainability.

Livestock systems play a major role in the gap between NUE_{crop} and NUE_{tot}. Of total current agricultural N loss estimated at 170 TgN, which is in line with a recent estimate[46], livestock production contributes 75% - loss from manure, grassland and cropland accounting for 28, 15 and 32% respectively. Consequently, current global average N loss factor is 11.4 per unit animal against 0.9 per unit vegetal protein. The decrease in the share of manure N recovered to cropland over the past decades (Supplementary Figure 7) highlights increasing disconnection and, thus, growing global challenges in closing nutrients loops between crop and livestock systems[47-49]. In Fig.3b, we stress that each boundary has different NUE_{tot} depending on NUE_{crop}, β and Y_{food}, and that, for a given food production boundary – meaning under constant production practices – NUE_{tot} decreases with α_{crops}.

Accordingly, decreasing the consumption of animal proteins and recoupling livestock and crop systems are essential conditions for reducing N pollution and addressing sustainability challenges. Unfortunately, planetary N sustainability targets are out of reach in B1 and B2 even with vegan diets, and are hard to achieve even in B3 despite N use efficiency being at maximum. This suggests that tackling N sustainability issues under industrial fertilization would possibly require a decrease in the share of cropland in favor of grassland. Such land use change is also acknowledged to support carbon sequestration and other ecosystem services, suggesting potential synergies for meeting sustainability targets[7,32,35,50]. However, cropland to grassland conversion would contrast with past trends and lower down the global feeding capacity. Under organic fertilization, B4 highlights that agricultural intensification without improvement in N use efficiency is incompatible with both food production and environmental sustainability challenges, and that increased N use efficiency as in B5 is a key condition for meeting these challenges. Accordingly, pollution mitigation requires integrated and multi-scale nutrient management strategies such as the adoption of best management practices at farm scale[51] and a system design involving synergies between crop and livestock farms in view of intensive nutrient pooling and recycling at landscape scale. Although ambitious, such goals are actionable through knowledge-based system planning, whose adoption supports climate change mitigation beyond the N cycle[50]. In contrast, N waste reduction through dietary change is socially more challenging because of global socioeconomic disparities. Indeed, reducing α_{crops} implies reducing global livestock production, which is likely to accentuate consumption inequalities between population groups in rich and poor countries[52] (Supplementary Figure 15). To tackle such risks and prevent environmental protection measures from accentuating inequalities or triggering food shocks, there is an increasing need for coordinated regulations and policy on food security and global sustainability challenges among countries.

In all simulations, Y_{food} and r_{loss} are complement fractions of N input even though the soil N pool might not always be constant in time. Indeed, N storage is controlled by soil conditions, land-use and management practices which are subject to change, but the way these factors combine into soil composition change is particularly hard to quantify at large spatiotemporal scales and is out of the scope of the present analysis. However, it can be argued that improved practices over time might have enabled potential N built-up in global soils, in particular grassland, but in contrast, the decline in the share of grassland through conversion to cropland over the last decades (τ decrease, Extended Data Figure 2f) might have backfired and offset such storage. Accordingly, r_{loss} trajectory from global agriculture might have been less regular than shown in our results due to inter-annual N stock change in relation to land-use change, which highlights that land management needs to integrate a long-term perspective.

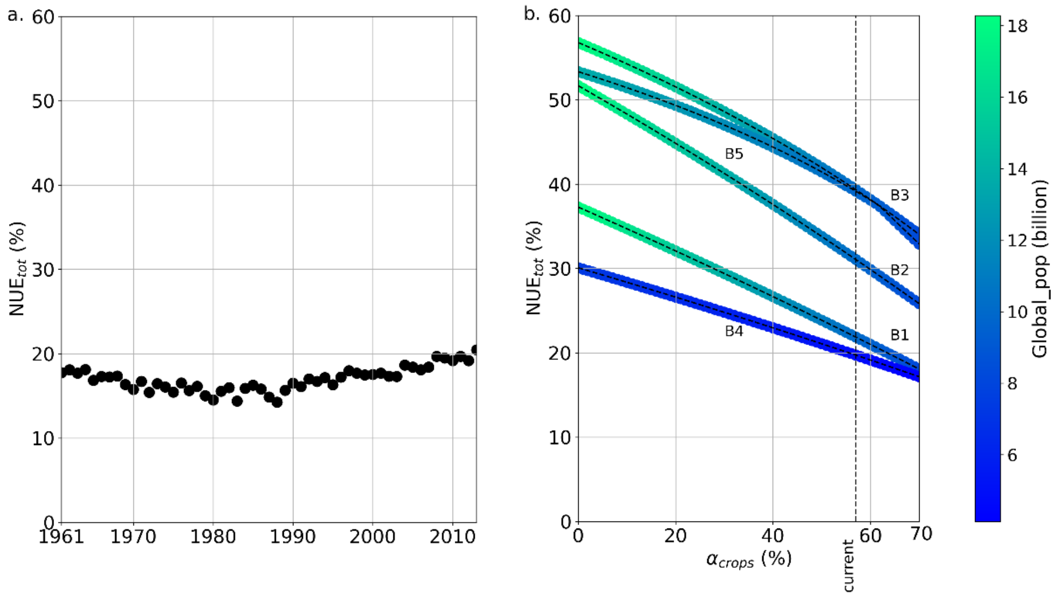

Fig.3| Total N use efficiency (NUE_{tot}) in global agriculture. a. NUE_{tot} over the benchmark period (1961-2013). b. NUE_{tot} in the five global food production boundaries (B1 to B5) in function of the share of crops used for feed (α_{crops}). NUE_{tot} is the ratio of food yield (Y_{food}) to the sum of Y_{food} and N loss rate (r_{loss}). For B4,B5, the calculation is done for the least N limitation (the highest Y_{food}) for each α_{crops}. The vertical dotted line indicates current global average α_{crops}. The color grid displays the feeding capacity ($Global_{pop}$) in B1-B5.

Growth rate challenges

We show in Fig.4 global average growth rates required to feed, by 2050, 10 billion people while respecting planetary N sustainability thresholds (blue and red lines for upper and medium threshold respectively). The growth required is lower than observed since 1961 for Y_{crop} and NCE, and slightly higher for Y_{grass}, whereas unprecedented efforts will be needed in NUE_{crop} and manure N recycling (β). NUE_{crop}, which is today highly variable across countries (Supplementary Figure 9) should increase globally as fast as observed in a handful of best performing countries over the last decades (Fig.4 and

Supplementary Figure 10, ref. [40]). In parallel, global weighted average β, which is currently in decline, should start increasing faster than Y_{crop}. To meet the medium threshold of N planetary sustainability, the share of grassland in global agricultural area should also increase and animal production decrease (Supplementary Table 4).

It would be groundless to position the organic boundaries (B4-B5) in Fig.4 for three reasons. First, although global certified organic land has doubled between 2010 and 2019 (ref. [53]), it still represents a tiny fraction of global agricultural area, i.e. ~1.5% – with grassland and cropland accounting for 83 and 17% respectively[53]. Second, there is lack of large-scale data on organic systems in particular regarding N cycling. Third, current organic systems receive considerable amounts of industrial N indirectly through manure recovered from non-organic systems[54]. Accordingly, we have refrained from defining the required growth rates of organic farming in the option space of these variables.

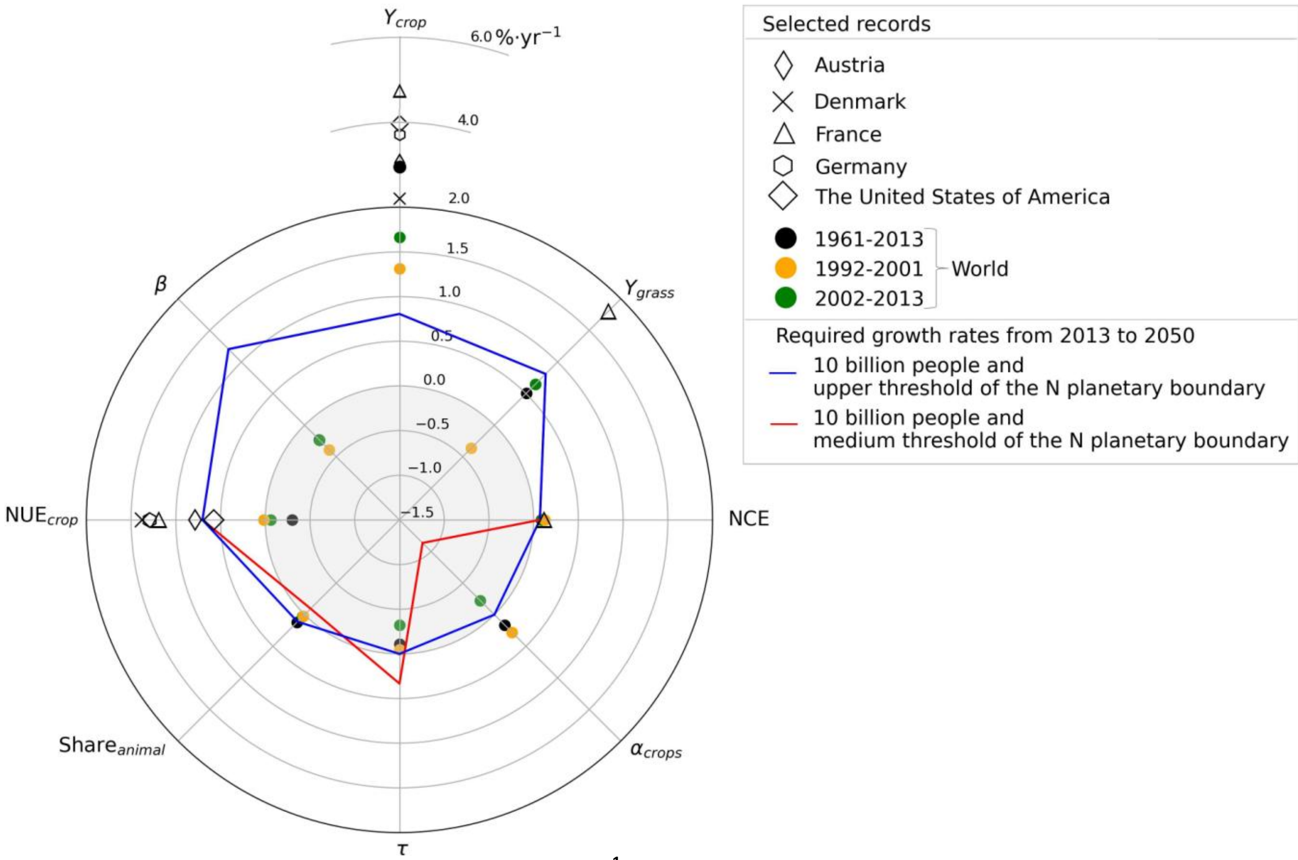

Fig. 4| Average non-compounding growth rates (%·yr^{-1}) required in key variables of global food production and N cycling to feed, by 2050, 10 billion people while staying within planetary sustainability thresholds. The blue and red lines respectively indicate the growth rates required to reach the upper and medium thresholds of planetary sustainability. The shown variables are the crop yield (Y_{crop}), grass yield (Y_{grass}), livestock nitrogen conversion efficiency (NCE), share of crops used for feed (α_{crops}), share of grassland in global agricultural area (τ), share of animal proteins in food supply ($Share_{animal}$), nitrogen use efficiency in cropland (NUE_{crop}) and the share of manure N recovered to cropland (β). All required rates are calculated for the period 2013-2050 (Supplementary Table 4) and are put in perspective with past global average and national-scale records considering the five best performing countries in terms of Y_{crop} and NUE_{crop} (Supplementary Table 5 and Supplementary Figure 10). The gray zone indicates negative rates.

Conclusion

Global food production and N loss are heading toward B1, and a synchronous increase in Y_{food} and NUE_{tot} will be a great challenge in the 21st century. Such a synchronous increase is all the more essential in organic farming to help closing Y_{food} gaps. The ongoing expansion in the demand for food and animal protein - while keeping today's total agricultural area constant - is subject to upper thresholds. We argue that demand beyond these thresholds is likely to further jeopardize planetary sustainability by driving up global agricultural land[55], N fertilizers use and loss[56]. Understanding the drivers of Y_{food} and NUE_{tot} allows the assessment of these upper thresholds and can provide useful insights for connecting population dynamics, land-use change and agricultural N cycling to the broad range of environmental sustainability challenges.

Methods

Model structure

The model builds on a set of 7 central equations that are analytically derived hereafter following a step-by-step presentation of all model variables. Equations 1-13 is the modelling system of the food yield (i.e. food production per unit total agricultural area) and global feeding capacity. Equations 14-29 is the modelling system of N cycling in support of production. Greek letters are used for variables representing shares and fractions. A flow diagram of the model is given in Extended Data Figure 1.

Food yield and production

The food yield (Y_{food}, $kgN \cdot ha^{-1} \cdot yr^{-1}$) is defined as total human-edible harvest (N_{food}, $kgN \cdot yr^{-1}$) per unit agricultural land (AL, ha).

$$Y_{food} = {}^{N_{food}}/_{AL} \qquad \text{(eq.1)}$$

AL is the sum of cropland and grassland. Cropland and grassland have highly uneven food production capacities. Harvest from grassland (N_{grass}, $kgN \cdot yr^{-1}$) is convertible into food only by livestock with efficiency of a few percent. Harvest from cropland (N_{crop}, $kgN \cdot yr^{-1}$) is directly human-edible and potential use of crop residues for feed ($N_{residues}$, $kgN \cdot yr^{-1}$) can increase food production from cropland.

N_{food} ($kgN \cdot yr^{-1}$) can be written as the sum of N_{grass}, N_{crop} and $N_{residues}$, plus livestock production ($N_{livestock}$, $kgN \cdot yr^{-1}$) minus total feed (N_{feed}, $kgN \cdot yr^{-1}$) (eq. 2). N_{feed} includes crops, residues and grass.

$$N_{food} = N_{crop} + N_{residues} + N_{grass} + N_{livestock} - N_{feed} \qquad \text{(eq. 2)}$$

N_{crop} is routed to feed ($N_{crops}^{livestock}$) and to uses other than feed (N_{crops}^{humans}) according to the share of crops used for feed (α_{crops}, %) following equations 3 to 5.

$$N_{crop} = N_{crops}^{humans} + N_{crops}^{livestock} \qquad \text{(eq. 3)}$$

$$N_{crops}^{humans} = Y_{crop} \times (1 - \alpha_{crops}) \times AL \times (1 - \tau) \qquad \text{(eq. 4)}$$

$$N_{crops}^{livestock} = Y_{crop} \times \alpha_{crops} \times AL \times (1 - \tau) \qquad \text{(eq. 5)}$$

where Y_{crop} ($kgN \cdot ha^{-1} \cdot yr^{-1}$) is the crop yield and τ (%) and (1-τ) (%) are respectively the shares of grassland and cropland in global agricultural area (AL).

N_{feed} is the sum of feed from grassland, cropland and residues and connects to $N_{livestock}$ according to livestock nitrogen conversion efficiency (NCE, %) (eq. 6, 7):

$$N_{feed} = N_{grass} + N_{crops}^{livestock} + N_{residues} \quad \text{(eq. 6)}$$

$$N_{livestock} = N_{feed} \times NCE \quad \text{(eq. 7)}$$

N_{grass} and $N_{residues}$ are calculated from equations 8 and 9:

$$N_{grass} = Y_{grass} \times \tau \times AL \quad \text{(eq. 8)}$$

$$N_{residues} = \left(\alpha_{residues} \times \frac{1-NHI}{NHI}\right) \times Y_{crop} \times (1-\tau) \times AL \quad \text{(eq. 9)}$$

where Y_{grass} ($kgN \cdot ha^{-1} \cdot yr^{-1}$) is the grass yield, $\alpha_{residues}$ (%) is the share of crop residues used for feed and NHI (%) is the harvest index of crops in terms of N, i.e. the ratio of N uptake in crop yield to the sum of N uptake in crop yield and crop residues.

Y_{food} can be written in equation 10 in function of the four positive drivers (Y_{crop}, Y_{grass}, NCE, $\alpha_{residues}$) and the two negative drivers (α_{crops}, τ).

$$Y_{food} = \left(NCE \times \left(\alpha_{residues} \times \frac{1-NHI}{NHI}\right) + 1\right) \times Y_{crop} \times (1-\tau) + NCE \times Y_{grass} \times \tau$$
$$+ \alpha_{crops} \times (1-\tau) \times Y_{crop} \times (NCE - 1) \quad \text{(eq. 10)}$$

We connect Y_{food} to food supply per hectare (Y_{food}^{supply}, $kgN \cdot ha^{-1} \cdot yr^{-1}$) i.e. the amount of Y_{food} available as food supply compared to seed and loss, from equations 11:

$$Y_{food}^{supply} = N_{food}^{supply} / AL = \left(\delta_{animal} \times N_{livestock} + \delta_{vegetal} \times N_{crops}^{humans}\right) / AL \quad \text{(eq. 11)}$$

where N_{food}^{supply} ($kgN \cdot yr^{-1}$) is total food supply, and $\delta_{vegetal}$ and δ_{animal} (%) are respectively the allocation shares of produced vegetal (N_{crops}^{humans}) and animal ($N_{livestock}$) proteins to food supply.

The share of animal proteins ($Share_{animal}$, %) in food supply is calculated from equation 12:

$$Share_{animal} = \delta_{animal} \times N_{livestock} / N_{food}^{supply} \quad \text{(eq.12)}$$

We calculate the global feeding capacity ($Global_{pop}$, inhabitants) by accounting for average food supply per capita (n_{food}^{supply}, $kgN \cdot cap^{-1} \cdot yr^{-1}$) following equation 13:

$$Global_{pop} = \delta_{weighted} \times Y_{food} \times AL / n_{food}^{supply} \quad \text{(eq. 13)}$$

where $\delta_{weighted}$ is the weighted average allocation of vegetal and animal proteins to food supply, i.e. $\delta_{weighted} \times Y_{food} = Y_{food}^{supply} = \left(\delta_{animal} \times N_{livestock} + \delta_{vegetal} \times N_{crops}^{humans}\right) / AL$.

The replacement of $\delta_{vegetal}$ and δ_{animal} by $\delta_{weighted}$ in equation 13 allows for consistently calculating $Global_{pop}$ in function of Y_{food}^{supply} and across a range of α_{crops} despite changing shares of vegetal and animal proteins in Y_{food}^{supply}.

N cycling

Total N input to agriculture (N_{tot}, $kgN \cdot yr^{-1}$) is the sum of food production (N_{food}, $kgN \cdot yr^{-1}$) and N loss (N_{loss}, $kgN \cdot yr^{-1}$) assuming no change in soil N pool, which is a common assumption in literature addressing large spatiotemporal scales[24,40,45].

$$N_{tot} = N_{food} + N_{loss} \quad \text{(eq. 14)}$$

Total N use efficiency (NUE_{tot}, %) is calculated with equation 15:

$$NUE_{tot} = {N_{food}} / {N_{tot}} \quad \text{(eq. 15)}$$

N_{tot} is the sum of biological nitrogen fixation (BNF, $kgN \cdot yr^{-1}$), atmospheric N deposition (N_{atm}, $kgN \cdot yr^{-1}$), industrial N fertilizers (N_{ind}, $kgN \cdot yr^{-1}$) and potential N return to agriculture via human excreta and food waste management ($N_{biowaste\_return}$, $kgN \cdot yr^{-1}$):

$$N_{tot} = BNF + N_{ind} + N_{atm} + N_{biowaste\_return} \quad \text{(eq. 16)}$$

Note that N_{tot} does not include livestock N excretion ($N_{excretion}$, $kgN \cdot yr^{-1}$) which is an internal agricultural flow.

$N_{biowaste\_return}$ is a fraction (ρ, %) of total food supply:

$$N_{biowaste\_return} = N_{food}^{supply} \times \rho \quad \text{(eq. 17)}$$

Input from BNF, N_{atm} and N_{ind} ($kgN \cdot yr^{-1}$) is the weighted sum of input rates ($kgN \cdot ha^{-1} \cdot yr^{-1}$) in cropland and grassland following equations 18-20, where weight is the share of grassland in global agricultural area (τ):

$$BNF = \left(r_{BNF}^{grass} \times \tau + r_{BNF}^{crop} \times (1 - \tau)\right) \times AL \quad \text{(eq. 18)}$$

where r_{BNF}^{grass} ($kgN \cdot ha^{-1} \cdot yr^{-1}$) and r_{BNF}^{crop} ($kgN \cdot ha^{-1} \cdot yr^{-1}$) are the BNF rates in grassland and cropland respectively.

$$N_{atm} = \left(r_{atm}^{grass} \times \tau + r_{atm}^{crop} \times (1 - \tau)\right) \times AL \quad \text{(eq. 19)}$$

where r_{atm}^{grass}($kgN \cdot ha^{-1} \cdot yr^{-1}$) and r_{atm}^{crop}($kgN \cdot ha^{-1} \cdot yr^{-1}$) are the N atmospheric deposition rates in grassland and cropland respectively.

$$N_{ind} = \left(r_{ind}^{grass} \times \tau + r_{ind}^{crop} \times (1-\tau)\right) \times AL \quad \text{(eq. 20)}$$

where r_{ind}^{grass}(kgN·ha^{-1}·yr^{-1}) and r_{ind}^{crop}(kgN·ha^{-1}·yr^{-1}) are the N industrial input rates in grassland and cropland respectively.

Livestock N excretion ($N_{excretion}$, kgN·yr^{-1}) is the difference between total feed (N_{feed}) and livestock production ($N_{livestock}$) and divides into N voided on grassland (N_{manure}^{grass}), N recovered as fertilizer in support of crops and residues production (N_{manure}^{crop} and $N_{manure}^{residues}$ respectively) and N loss from manure (N_{manure}^{loss}). We assume that N_{manure}^{grass} is a fraction (γ, %) of N feed from grassland (N_{grass}) and that $N_{manure}^{residues}$ equals N feed from residues ($N_{residues}$). The difference between $N_{excretion}$ and the sum of N_{manure}^{grass} and $N_{manure}^{residues}$ divides into N_{manure}^{crop} and N_{manure}^{loss}. β is the ratio of N_{manure}^{crop} to the sum of N_{manure}^{crop} and N_{manure}^{loss}. The N balance of total excretion follows equations 21 to 25:

$$N_{excretion} = N_{manure}^{grass} + N_{manure}^{residues} + N_{manure}^{crop} + N_{manure}^{loss} \quad \text{(eq. 21)}$$

$$N_{manure}^{grass} = (1 - NCE) \times N_{grass} \times \gamma \quad \text{(eq. 22)}$$

$$N_{manure}^{residues} = N_{residues} \quad \text{(eq. 23)}$$

$$N_{manure}^{crop} = ((1 - NCE) \times \left(N_{crops}^{livestock} + N_{residues} + N_{grass} \times (1-\gamma)\right) - N_{residues}) \times \beta \quad \text{(eq. 24)}$$

$$N_{manure}^{loss} = ((1 - NCE) \times \left(N_{crops}^{livestock} + N_{residues} + N_{grass} \times (1-\gamma)\right) - N_{residues}) \times (1-\beta) \quad \text{(eq. 25)}$$

where NCE (%) is livestock nitrogen conversion efficiency.

Y_{grass} (kgN·ha^{-1}·yr^{-1}) and N loss per unit grassland (r_{grass}^{loss}, kgN·ha^{-1}·yr^{-1}) connect to N input according to N use efficiency in grassland (NUE_{grass}, %) (eq. 26-27):

$$Y_{grass} = NUE_{grass} \times \left(r_{BNF}^{grass} + r_{atm}^{grass} + r_{ind}^{grass} + \frac{N_{manure}^{grass}}{\tau \times AL}\right) \quad \text{(eq. 26)}$$

$$r_{grass}^{loss} = \left(1 - NUE_{grass}\right) \times (Y_{grass}/NUE_{grass}) \quad \text{(eq. 27)}$$

Y_{crop} (kgN·ha^{-1}·yr^{-1}) and N loss per unit cropland (r_{crop}^{loss}, kgN·ha^{-1}·yr^{-1}) connect to N input according to N use efficiency in cropland (NUE_{crop}, %) (eq. 28-29):

$$Y_{crop} = NUE_{crop} \times \left(r_{BNF}^{crop} + r_{atm}^{crop} + r_{ind}^{crop} + \frac{N_{manure}^{crop} + N_{biowaste\_return}}{(1-\tau) \times AL}\right) \quad \text{(eq. 28)}$$

$$r_{crop}^{loss} = \left(1 - NUE_{crop}\right) \times (Y_{crop}/NUE_{crop}) \quad \text{(eq. 29)}$$

Average N loss per unit global agricultural area (r_{loss}, kgN·ha^{-1} ·yr^{-1}) is calculated from equation 30:

$$r_{loss} = r_{crop}^{loss} \times (1-\tau) + r_{grass}^{loss} \times \tau + N_{manure}^{loss}/AL \quad \text{(eq. 30)}$$

From equations 14-30, we derive equations 31-34.

$$Y_{grass} = {NUE_{grass} \times \left(r_{BNF}^{grass} + r_{atm}^{grass} + r_{ind}^{grass}\right)} \Big/ {\left(1 - NUE_{grass} \times (1 - NCE) \times \gamma\right)} \qquad \text{(eq. 31)}$$

$$Y_{crop} = \frac{NUE_{crop} \times \left(r_{BNF}^{crop} + r_{atm}^{crop} + r_{ind}^{crop} + \ (1 - NCE) \times \ Y_{grass} \times \ \tau \times \dfrac{(1-\gamma)}{(1-\tau)} \times \beta + {Y_{food}^{supply} \ \times \ \rho} \Big/ {(1-\tau)} \right)}{1 - NUE_{crop} \times \beta \times \left((1 - NCE) \times \alpha_{crops} - NCE \times \left(\alpha_{residues} \times \dfrac{1 - NHI}{NHI} \right) \right)}$$

$$\text{(eq. 32)}$$

$$NUE_{tot} = {Y_{food}} \Big/ {\left((r_{BNF}^{grass} + r_{ind}^{grass} + r_{atm}^{grass}) \times \tau + (r_{BNF}^{crop} + r_{ind}^{crop} + r_{atm}^{crop}) \times (1-\tau) + Y_{food}^{supply} \ \times \ \rho \right)} \qquad \text{(eq. 33)}$$

$$r_{loss} = (1 - NUE_{tot}) \times \left((r_{BNF}^{grass} + r_{ind}^{grass} + r_{atm}^{grass}) \times \tau + (r_{BNF}^{crop} + r_{ind}^{crop} + r_{atm}^{crop}) \times (1-\tau) + Y_{food}^{supply} \ \times \ \rho \right) \qquad \text{(eq. 34)}$$

Equations 10, 12-13 and 31-34 are the 7 central model equations.

Model variables classification and model calibration

Equations 10, 12-13 and 31-34 allow calculating 7 model output variables with 21 input variables. We simulate global food production and N cycling over the benchmark period 1961-2013, and in five global food production boundaries. The next subsections present the data used in the simulations. Of the 7 model output variables, 5 are common to all simulations (benchmark period and B1-B5). These are the food yield (Y_{food}), the share of animal proteins in diets ($Share_{animal}$), global feeding capacity ($Global_{pop}$), N loss rate (r_{loss}), and total N use efficiency (NUE_{tot}). Over the benchmark period, the 2 additional model output variables are the biological N fixation rate in grassland (r_{BNF}^{grass}) and N use efficiency in cropland (NUE_{crop}). In B1-B3 (unconstrained industrial fertilization), the 2 additional model output variables are the industrial N input rates in cropland (r_{ind}^{crop}) and grassland (r_{ind}^{grass}). In B4-B5 (organic fertilization), the 2 additional model output variables are the crop yield (Y_{crop}) and grass yield (Y_{grass}). Note that in this case Y_{crop} is recursive by depending on N_{food}^{supply} through ρ. The resolution of the modeling system in B4-B5 requires two steps. First, we calculate Y_{crop} and Y_{food}^{supply} for ρ=0, then we inject the result in the modelling system and recalculate Y_{food}^{supply}.

In the following subsection, we specify the classification of model variables between input and output in each simulation and present the model calibration. Full data series over the benchmark period are shown in Extended Data Figures 2-3 and Supplementary Figures 1-8. Extended Data Tables 2,3 summarize, on the one hand, the classification of model variables between input and output, and, on the other hand, global weighted average data in 1961 and 2013 (Extended Data Table 2) and in B1-B5 (Extended Data Table 3a,b). Sensitivity analysis of the model is addressed in Supplementary Figures 11-13.

Food yield and production

Crop yield (Y_{crop}). Over the benchmark period, Y_{crop} is a model input variable (Extended Data Figure 2a). It is calculated from global average yield of individual crops weighted by crop area[33] and N content of crops[57,58] .

In B1-B3, where industrial N fertilizers ensure a full closure of crop yield gaps worldwide[27], Y_{crop} is a model input variable set at 74 $kgN \cdot ha^{-1} \cdot yr^{-1}$ (Supplementary Table 2), which is the global weighted upper threshold of Y_{crop} given worldwide biophysical constraints and crop mix. Crops that are not reported in ref. [27] cover 29% of total cropland in 2013. We apply crop yield gaps of reported crops to all crops. In B4-B5, Y_{crop} is a model output variable calculated in function of N cycling. Supplementary Figure 11g,h provides model sensitivity analysis on Y_{crop}.

Share of crops used for feed (α_{crops}). Over the benchmark period, α_{crops} is calculated from FAO commodity balance sheets as the ratio of crops used for feed ($\mathrm{N}_{\mathrm{crops}}^{\mathrm{livestock}}$) to total crops production (excluding residues). We calculate $\mathrm{N}_{\mathrm{crops}}^{\mathrm{livestock}}$ across all FAOSTAT crop categories i as the difference in terms of N between total crop production ($Prod_i$) and the sum of food supply ($Supply_i$), seed ($Seed_i$), other uses (such as soap, pet food) ($Other_i$) and food loss ($Loss_i$). Because the N content of primary crops and final products are different, we use a set of reference N contents for primary crops[58] ($\mathrm{N}_{\mathrm{i}}^{\mathrm{prod}}$) that we also apply to seed and a set of N contents for food supply[34] ($\mathrm{N}_{\mathrm{i}}^{\mathrm{supply}}$) that we also apply to food loss:

$$\mathrm{N}_{\mathrm{crops}}^{\mathrm{livestock}} = \sum_{\mathrm{i}} \left(\mathrm{Prod}_{\mathrm{i}} \times \mathrm{N}_{\mathrm{i}}^{\mathrm{prod}} - (\mathrm{Supply}_{\mathrm{i}} + \mathrm{Loss}_{\mathrm{i}}) \times \mathrm{N}_{\mathrm{i}}^{\mathrm{supply}} - (\mathrm{Seed}_{\mathrm{i}} + \mathrm{Other}_{\mathrm{i}}) \times \mathrm{N}_{\mathrm{i}}^{\mathrm{prod}} \right)$$

α_{crops} over the benchmark period is shown in Extended Data Figure 2b.

In B1-B5, α_{crops} is a model input variable set to range from 0 to 70%. α_{crops} of 0 means no feed-food competition, and implies that animal proteins in diets are exclusively supplied by ruminants fed on grassland and crop residues. As a condition that maximizes feed conversion to food, α_{crops} in B1-B5 is allocated to meat from monogastrics and dairy production which have higher N conversion efficiency than meat from ruminants (see respective subsection below).

Grassland yield (Y_{grass}), N harvest index of crops (NHI) and the share of crop residues used for feed ($\alpha_{residues}$). Grass and crop residues used for feed are not reported in FAOSTAT. Their sum equals total feed minus feed from crops. Over the benchmark period, feed from crops is reported in FAOSTAT and total feed is calculated as the sum of $\mathrm{N}_{\mathrm{livestock}}$ and $\mathrm{N}_{\mathrm{excretion}}$ derived from ref. [33]. The amount of residues used for feed is a fraction of total residues production. We calculate total residues production from crops production using constant NHI of 70% over the benchmark period. NHI is calculated by considering global weighted average harvest index of 42% in terms of mass (ref. [59]) and N contents in grain and crop residues of 1.9% and 0.6% respectively[57,59]. Due to uncertainty in global crop residues use over the benchmark period, the fraction used for feed ($\alpha_{residues}$) is assumed to vary between the current value of 30% (ref. [24]) and an asymptotic decline from 70 in 1961 to 30% today (Extended Data Figure 2c,d). The breakdown of total feed among crops, grass and crop residues is shown in Extended Data Figure 3a. Global average Y_{grass} is calculated by dividing feed from grassland by grassland area.

In B1-B5, NHI and $\alpha_{residues}$ are kept constant at respectively 70% and 30% as in 2013 (see Supplementary discussion and sensitivity analysis in Supplementary Figure 11a-d). In contrast to Y_{crop}, Y_{grass} is poorly documented in the scientific literature. In B1-B3, global weighted Y_{grass} is a model input variable set at 29 $kgN \cdot ha^{-1} \cdot yr^{-1}$, which is 30% above current (2013) level. Such increase is ambitious given the majority of semi-natural areas in global grassland[30]. In Supplementary Figure 10i,j, we provide model sensitivity analysis on Y_{grass}. In B4-B5, Y_{grass} is a model output variable simulated in function of N availability under N limitation.

Livestock nitrogen conversion efficiency (NCE). Over the benchmark period, NCE is a model input variable calculated as the ratio of $N_{livestock}$ to N_{feed} from ref. [33]. Seafood is excluded. Global average NCE has doubled from 4.1 in 1961 to 8.7% in 2013 (Extended Data Figure 2e).

In B1-B5, global aggregate NCE is a model input variable. Upper bounds to NCE are specific to animal products[31], meaning that global aggregate NCE depends on improvements in animal breeding but also on choice of animal proteins in diets. In B1-B5, we assume product-specific NCE of 15% for monogastrics[60] (pork, poultry and eggs) and dairy production and 5% for ruminants meat[31], and set the global upper threshold for aggregate NCE at 11.2%. This threshold is more ambitious than previous estimates[61] and is 30% above current NCE. We address model sensitivity analysis on NCE in Supplementary Figure 10e,f and Supplementary discussion.

Global agricultural area (AL) and the share of grassland in global agricultural area (τ). AL is the sum of grassland and all harvested cropland (excluding fibers which account for less than 3%). Grassland is the sum of permanent meadows and pasture, temporary meadows and pasture, temporary fallow land and fodder legumes. Over the benchmark period, data on cropland and grassland are from FAOSTAT (ref. [33]) except for fodder legumes which are not reported and are considered constant at 90 Mha (ref. [62]). Over the benchmark period, τ is a model input variable calculated annually (Extended Data Figure 2f, Supplementary Figure 1, Supplementary Table 1).

In B1-B5, AL is equal to year 2013 and τ is a model input variable reflecting potential change in global grassland-to-cropland allocation. The feeding capacity increases inversely to τ due to higher human-edible yield of cropland compared to grassland. Starting with current (2013) global τ of 72.3%, we consider τ decrease to 70.2%, which equates to 100 Mha conversion of grassland to cropland (8% increase in global cropland). This number exceeds the latest FAOSTAT projection[63] of 11 Mha (see Supplementary discussion).

Global average food yield (Y_{food}) allocation and average food supply per capita (n_{food}^{supply}). Over the benchmark period, Y_{food} as reconstructed annually from equation 10 is validated on FAOSTAT data. After validation, global weighted average Y_{food} is allocated between food supply, seed, other uses and food losses (Supplementary Figure 2) by considering annual allocation shares for vegetal ($\delta_{vegetal}$) and animal proteins (δ_{animal}). Average $\delta_{vegetal}$ and δ_{animal} over the benchmark period are respectively 69% and 98% (ref. [33]). The calculated annual Y_{food}, food supply and its content in animal proteins are smoothened over time assuming global harvest variability absorption through interannual stocks. Global average food supply per capita (n_{food}^{supply}) excluding seafood allows connecting food availability to global population, and has increased from 3.43 $kgN \cdot cap^{-1} \cdot yr^{-1}$ in 1961 to 4.43 $kgN \cdot cap^{-1} \cdot yr^{-1}$ in 2013 (ref. [33] and Supplementary Figure 3).

In B1-B5, we assume global weighted average allocation ($\delta_{weighted}$) of Y_{food} to Y_{food}^{supply} equal to 72% which is the weighted average $\delta_{vegetal}$ and δ_{animal} in 2013. Global weighted average n_{food}^{supply} in B1-B5 is also assumed identical to 2013 i.e. 4.43 $kgN \cdot cap^{-1} \cdot yr^{-1}$. The supply of calories is out of the scope of the paper.

N cycling

Atmospheric N deposition (N_{atm}). Over the benchmark period, N_{atm} on agricultural land is a model input variable. N_{atm} represents N deposition resulting from emissions (in particular NO_x) of non-agricultural sectors. Global NO_x emissions from non-agricultural sectors have increased by 60% over the period[64]. Accordingly, N_{atm} is reconstructed by considering a baseline global average atmospheric deposition rate in cropland ($\mathrm{r}_{\mathrm{atm}}^{\mathrm{crop}}$) and grassland ($\mathrm{r}_{\mathrm{atm}}^{\mathrm{grass}}$) of 5kgN·ha^{-1}·yr^{-1} in 1961 (ref. [52]) and a linear increase to 8 kgN·ha^{-1}·yr^{-1} (60% increase) to 2013. In B1-B5, $\mathrm{r}_{\mathrm{atm}}^{\mathrm{crop}}$ and $\mathrm{r}_{\mathrm{atm}}^{\mathrm{grass}}$ are model input variables considered equal to 8 kgN·ha^{-1}·yr^{-1} as in year 2013.

Industrial N fertilizer (N_{ind}). Over the benchmark period, N_{ind} is a model input variable derived from FAOSTAT (ref. [1] and Supplementary Figure 6). FAOSTAT does not report separately N_{ind} application on grassland and cropland. For recent years, the share of N_{ind} applied to global grassland is reported at 4.6% (ref. [65]). We assume the same share in 1961 which is consistent with constant share of N_{ind} applied to grassland over the period 1961-2013 reported for Europe (ref. [66]). Based on this, we derive N_{ind} fertilization rates (kgN·ha^{-1}·yr^{-1}) in cropland ($\mathrm{r}_{\mathrm{ind}}^{\mathrm{crop}}$) and grassland ($\mathrm{r}_{\mathrm{ind}}^{\mathrm{grass}}$) over the benchmark period (Supplementary Figure 5).

In B1-B3, $\mathrm{r}_{\mathrm{ind}}^{\mathrm{crop}}$ and $\mathrm{r}_{\mathrm{ind}}^{\mathrm{grass}}$ are model output variables. In B4-B5, $\mathrm{r}_{\mathrm{ind}}^{\mathrm{crop}}$ and $\mathrm{r}_{\mathrm{ind}}^{\mathrm{grass}}$ are null by definition.

Global average biological nitrogen fixation (BNF) rates in cropland ($\mathrm{r}_{\mathrm{BNF}}^{\mathrm{crop}}$) and grassland ($\mathrm{r}_{\mathrm{BNF}}^{\mathrm{grass}}$). Over the benchmark period, $\mathrm{r}_{\mathrm{BNF}}^{\mathrm{crop}}$ is reconstructed in function of global weighted average crop yield for fixing crops (soybean, groundnuts and pulses) using the methodology in Lassaletta et al. (ref. [40]), and includes green manures of 2.2 TgN (ref. [62]) and fixation rates of 25 and 33 kgN·ha^{-1}·yr^{-1} for sugarcane and rice respectively[67]. $\mathrm{r}_{\mathrm{BNF}}^{\mathrm{crop}}$ is shown over the benchmark period in Supplementary Figure 4 and is 24.8 kgN·ha^{-1}·yr^{-1} in 2013. $\mathrm{r}_{\mathrm{BNF}}^{\mathrm{grass}}$ is not recorded over the benchmark period and is a model output variable (Supplementary Figure 4).

In B1-B3, $\mathrm{r}_{\mathrm{BNF}}^{\mathrm{crop}}$ and $\mathrm{r}_{\mathrm{BNF}}^{\mathrm{grass}}$ do not affect Y_{food} thanks to unconstrained N_{ind}, and are model input variables equal to year 2013. In contrast, in B4-B5, $\mathrm{r}_{\mathrm{BNF}}^{\mathrm{crop}}$ and $\mathrm{r}_{\mathrm{BNF}}^{\mathrm{grass}}$ are critical to Y_{food} (due to banned N_{ind}) and are model input variables assigned improvements assumed feasible at the global scale. We assume these improvements to rely on more green manures and fodder legumes cultivation in global cropland and grassland. Because in our model fallow land, temporary meadows and fodder legumes are classified as grassland, fodder legumes plantation in these land systems is the main lever of global BNF intensification. We calculate improved $\mathrm{r}_{\mathrm{BNF}}^{\mathrm{grass}}$ by assuming the plantation of all global fallow land estimated at ~100 Mha (ref. [33]) with fodder legumes fixing 125 kgN·ha^{-1}·yr^{-1} throughout the year. In addition, we assume that half of global cropland enters rotations with temporary grassland and fodder legumes fixing 125 kgN·ha^{-1}·yr^{-1} over multiannual cycles. The frequency of fixing crops in these cycles is assumed to be of 2 years within 8 year rotations, resulting in average annual fixation rate of about 30 kgN·ha^{-1}·yr^{-1} over 690 Mha of global agricultural area. In sum, $\mathrm{r}_{\mathrm{BNF}}^{\mathrm{grass}}$ in B4-B5 is increased from currently 10.2 kgN·ha^{-1}·yr^{-1} (year 2013) to 18 kgN·ha^{-1}·yr^{-1} which adds 26 TgN·yr^{-1} compared to 2013. In addition to BNF intensification through fodder legumes, BNF intensification in cropland also assumes a fourfold increase in green manures from currently 2.2 to 8.8 TgN·yr^{-1}, which is consistent with the detailed analysis in Smil (ref. [62]). In sum, $\mathrm{r}_{\mathrm{BNF}}^{\mathrm{crop}}$ in B4-B5 is increased from currently 24.8 kgN·ha^{-1}·yr^{-1} to 30 kgN·ha^{-1}·yr^{-1}, and total BNF in global agricultural area is increased from 69 to 102 TgN·yr^{-1}.

Fraction of N voided on grassland (γ). There are no reliable large-scale literature estimates for γ. Both over the benchmark period and in B1-B5, γ is a model input variable equal to 50%. Model sensitivity analysis for γ is addressed in Supplementary Figure 11n-p.

Share of biowaste N return to agriculture (ρ) via human excreta and food waste management. There are no global estimates for ρ, and scarce available studies like for China suggest a sharp decrease over the last decades[68]. Over the benchmark period, we assume a linear decrease in ρ from 30% to 5%. In B1-B3, where industrial N fertilizers ensure no N limitation, ρ is equal to 5% as in 2013. In B4-B5, ρ is a model input variable set to range from 5% to 30% (see Supplementary discussion).

Nitrogen use efficiency in cropland (NUE_{crop}). Over the benchmark period, NUE_{crop} is a model output variable. Although upper thresholds for NUE_{crop} are unclear, historical trajectories at the scale of countries indicate that NUE_{crop} improves with agricultural practices and, in rare cases, tends toward an asymptote at around 70% (ref. [40] and Supplementary Figure 9). Only a handful of countries (Austria, Denmark, France, Germany and USA) have managed to achieve this asymptote while maintaining crop yields above 70 $kgN \cdot ha^{-1} \cdot yr^{-1}$ (Supplementary Figure 10). In B1 and B4, NUE_{crop} is assumed equal to year 2013. In B2, B3 and B5, NUE_{crop} is set at 70%, which is very ambitious at the global scale.

Nitrogen use efficiency in grassland (NUE_{grass}). NUE_{grass} is barely documented in the scientific literature. Both over the benchmark period and in B1-B5, NUE_{grass} is a model input variable that we assume constant at 75%. We address model sensitivity analysis on NUE_{grass} in Supplementary Figure 11k-m.

Share of manure N recovery to cropland (β). Over the benchmark period, β is a model input variable (Supplementary Figure 7) calculated by combining N balance between N_{feed} and $N_{excretion}$ with data reporting manure applied to soils[33].

In B1-B2 and B4, β is assumed equal to 35% as in 2013. In B3 and B5, β is set at 80% which has recently been suggested as an upper limit[69].

Uncertainty

The modeling system totals 28 variables, and allows simulating 7 output variables. Except for 4 model variables for which long-term global data are not available (NHI, γ, ρ, NUE_{grass}), all model input variables (16 in each simulation) are calibrated over a benchmark period of half a century (1961-2013) using best available literature estimates and global weighted average FAOSTAT data (Extended Data Figure 2,3 and Supplementary Figures 1-9). Model calibration on long data series reduces uncertainty and, in addition, simulations integrate minimum-maximum ranges for key model input variables (α_{crops}, τ, r_{BNF}^{crop}, r_{BNF}^{grass}, NUE_{crop}, β, and ρ). Further, model sensitivity is addressed for individual variables (one-at-a-time) in Supplementary Figure 11 and for all model input variables combined through Monte Carlo simulations (Supplementary Figure 12 for B1-B3 and Supplementary Figure 13 for B4-B5).

Planetary N sustainability thresholds

Allowable N loss from global agriculture to remain within planetary N sustainability thresholds[3,4,70] is reported between 50 and 100 TgN (ref. [24]). Expressed per hectare of global agricultural area, the allowable global average N loss rate (r_{loss}) is between 10.5 and 21 $kgN \cdot ha^{-1} \cdot yr^{-1}$, with medium at 15.5 $kgN \cdot ha^{-1} \cdot yr^{-1}$. The above 3 r_{loss} values are adopted respectively as the lower, upper and medium thresholds of planetary N sustainability.

Data availability

The bulk of input data used in the analysis is derived from the statistics of the United Nations Food and Agriculture Organization (FAO), available at: http://www.fao.org/faostat/en/#data. The N content coefficients of primary crops are taken from Lassaletta et al. (ref. [58]) and the N content coefficients of food supply are from FAOSTAT Food Balance Sheets (ref. [34]). Data on crop yield gaps are taken from Mueller et al. (ref. [27]). Other data sources are specified in Methods.

Code availability

The code developed in the study is available from the corresponding author upon reasonable request.

Acknowledgements

The work was developed with funding from the research program Emergence Ville de Paris Convention 2015 DDEES 165. The authors would like to thank Thomas Gregor for valuable stylistic remarks on a previous version of the manuscript.

Author Contributions Statement

Both authors conceived and designed the study, analyzed and interpreted the data, defined the Methods, developed the ALPHA model, discussed the ideas and results, and wrote and revised the paper.

Competing Interests Statement

The authors declare no competing interest.

References

1. Foley, J. A. *et al.* Solutions for a cultivated planet. *Nature* **478**, 337–342 (2011).
2. Klein Goldewijk, K., Beusen, A., Doelman, J. & Stehfest, E. Anthropogenic land use estimates for the Holocene – HYDE 3.2. *Earth Syst. Sci. Data* **9**, 927–953 (2017).
3. Steffen, W. *et al.* Planetary boundaries: Guiding human development on a changing planet. *Science* **347**, 1259855–1259855 (2015).
4. Rockström, J. *et al.* A safe operating space for humanity. *Nature* **461**, 472–475 (2009).
5. Erb, K.-H. *et al.* Exploring the biophysical option space for feeding the world without deforestation. *Nat. Commun.* **7**, 11382 (2016).

6. Ramankutty, N. *et al.* Trends in Global Agricultural Land Use: Implications for Environmental Health and Food Security. *Annu. Rev. Plant Biol.* **69**, 789–815 (2018).
7. Foley, J. A. Global Consequences of Land Use. *Science* **309**, 570–574 (2005).
8. Tilman, D., Cassman, K. G., Matson, P. A., Naylor, R. & Polasky, S. Agricultural sustainability and intensive production practices. *Nature* **418**, 671–677 (2002).
9. Krausmann, F. *et al.* Global human appropriation of net primary production doubled in the 20th century. *Proc. Natl. Acad. Sci.* **110**, 10324–10329 (2013).
10. Galloway, J. N. *et al.* The Nitrogen Cascade. *BioScience* **53**, 341–356 (2003).
11. Smil, V. *Enriching the earth: Fritz Haber, Carl Bosch, and the transformation of world food production*. (MIT, 2001).
12. Erisman, J. W., Sutton, M. A., Galloway, J., Klimont, Z. & Winiwarter, W. How a century of ammonia synthesis changed the world. *Nat. Geosci.* **1**, 636–639 (2008).
13. Smil, V. Nitrogen and Food Production: Proteins for Human Diets. *AMBIO J. Hum. Environ.* **31**, 126–131 (2002).
14. Vitousek, P. M. *et al.* Human Alteration of the Global Nitrogen Cycle: Sources and Consequences. *Ecol. Appl.* **7**, 737–750 (1997).
15. Sutton, M. A. *et al. The European nitrogen assessment: sources, effects and policy perspectives*. (Cambridge Univ. Press, 2011).
16. Cohen, J. E. *How many people can the Earth support?* (Norton, 1995).
17. Malthus, T. R. *First Essay on Population 1798*. (Palgrave Macmillan UK, 1966). doi:10.1007/978-1-349-81729-0.
18. Harchaoui, S. & Chatzimpiros, P. Energy, Nitrogen, and Farm Surplus Transitions in Agriculture from Historical Data Modeling. France, 1882-2013.: Energy, Nitrogen, and Farm Surplus Transitions. *J. Ind. Ecol.* (2018) doi:10.1111/jiec.12760.
19. Van Den Bergh, J. C. J. M. & Rietveld, P. Reconsidering the Limits to World Population: Meta-analysis and Meta-prediction. *BioScience* **54**, 195 (2004).
20. Cohen, J. E. How many people can the Earth support? *J. Popul. Sustain.* **2**, 37–42 (2017).
21. Barbieri, P. *et al.* Global option space for organic agriculture is delimited by nitrogen availability. *Nat. Food* **2**, 363–372 (2021).
22. Billen, G. *et al.* Reshaping the European agro-food system and closing its nitrogen cycle: The potential of combining dietary change, agroecology, and circularity. *One Earth* **4**, 839–850 (2021).
23. UNDESA. *World Population Prospects: The 2022 Revision, Key Findings and Advance Tables.* (2022).
24. Bodirsky, B. L. *et al.* Reactive nitrogen requirements to feed the world in 2050 and potential to mitigate nitrogen pollution. *Nat. Commun.* **5**, (2014).
25. Dupas, M.-C., Halloy, J. & Chatzimpiros, P. Power law scaling and country-level centralization of global agricultural production and trade. *Environ. Res. Lett.* (2022) doi:10.1088/1748-9326/ac54ca.
26. D'Odorico, P., Carr, J. A., Laio, F., Ridolfi, L. & Vandoni, S. Feeding humanity through global food trade. *Earths Future* **2**, 458–469 (2014).
27. Mueller, N. D. *et al.* Closing yield gaps through nutrient and water management. *Nature* **490**, 254–257 (2012).
28. Daioglou, V., Stehfest, E., Wicke, B., Faaij, A. & Vuuren, D. P. van. Projections of the availability and cost of residues from agriculture and forestry. *GCB Bioenergy* **8**, 456–470 (2016).
29. Oenema, O., de Klein, C. & Alfaro, M. Intensification of grassland and forage use: driving forces and constraints. *Crop Pasture Sci.* **65**, 524 (2014).

30. Fetzel, T. *et al.* Quantification of uncertainties in global grazing systems assessment: Uncertainties in Global Grazing Data. *Glob. Biogeochem. Cycles* **31**, 1089–1102 (2017).
31. Smil, V. *Feeding the world: a challenge for the twenty-first century*. (MIT Press, 2000).
32. Bengtsson, J. *et al.* Grasslands-more important for ecosystem services than you might think. *Ecosphere* **10**, e02582 (2019).
33. FAOSTAT. *FAO statistical database*. http://www.fao.org/faostat/en/#data/RL (2018).
34. FAOSTAT FBS. FAOSTAT Food Balance Sheet. *FAOSTAT Food Balance Sheet* http://www.fao.org/faostat/en/#data/FBS (2021).
35. Lemaire, G. *Grassland productivity and ecosystem services*. (CABI, 2011). doi:10.1079/9781845938093.0000.
36. Tilman, D., Wedin, D. & Knops, J. Productivity and sustainability influenced by biodiversity in grassland ecosystems. *Nature* **379**, 718–720 (1996).
37. OECD & Food and Agriculture Organization of the United Nations. *OECD-FAO Agricultural Outlook 2020-2029*. (OECD, 2020). doi:10.1787/1112c23b-en.
38. Mottet, A. *et al.* Livestock: On our plates or eating at our table? A new analysis of the feed/food debate. *Glob. Food Secur.* **14**, 1–8 (2017).
39. Bai, Z. *et al.* China's livestock transition: Driving forces, impacts, and consequences. *Sci. Adv.* **4**, eaar8534 (2018).
40. Lassaletta, L., Billen, G., Grizzetti, B., Anglade, J. & Garnier, J. 50 year trends in nitrogen use efficiency of world cropping systems: the relationship between yield and nitrogen input to cropland. *Environ. Res. Lett.* **9**, 105011 (2014).
41. Smil, V. Eating Meat: Evolution, Patterns, and Consequences. *Popul. Dev. Rev.* **28**, 599–639 (2002).
42. Connor, D. J. Organic agriculture and food security: A decade of unreason finally implodes. *Field Crops Res.* **225**, 128–129 (2018).
43. Muller, A. *et al.* Strategies for feeding the world more sustainably with organic agriculture. *Nat. Commun.* **8**, (2017).
44. Willett, W. *et al.* Food in the Anthropocene: the EAT–Lancet Commission on healthy diets from sustainable food systems. *The Lancet* **393**, 447–492 (2019).
45. Zhang, X. *et al.* Managing nitrogen for sustainable development. *Nature* (2015) doi:10.1038/nature15743.
46. Conijn, J. G., Bindraban, P. S., Schröder, J. J. & Jongschaap, R. E. E. Can our global food system meet food demand within planetary boundaries? *Agric. Ecosyst. Environ.* **251**, 244–256 (2018).
47. Cowling, E. B. & Galloway, J. N. Challenges and opportunities facing animal agriculture: Optimizing nitrogen management in the atmosphere and biosphere of the Earth1. *J. Anim. Sci.* **80**, E157–E167 (2002).
48. Naylor, R. *et al.* Losing the Links Between Livestock and Land. *Science* **310**, 1621–1622 (2005).
49. Uwizeye, A. *et al.* Nitrogen emissions along global livestock supply chains. *Nat. Food* **1**, 437–446 (2020).
50. Xia, L., Lam, S. K., Yan, X. & Chen, D. How Does Recycling of Livestock Manure in Agroecosystems Affect Crop Productivity, Reactive Nitrogen Losses, and Soil Carbon Balance? *Environ. Sci. Technol.* **51**, 7450–7457 (2017).
51. Xia, L. *et al.* Can knowledge-based N management produce more staple grain with lower greenhouse gas emission and reactive nitrogen pollution? A meta-analysis. *Glob. Change Biol.* **23**, 1917–1925 (2017).
52. Downs, S. M. & Fox, E. L. Uneven decline in food system inequality. *Nat. Food* **2**, 141–142 (2021).

53. FiBL. Area data on organic agriculture worldwide 2008-2019. https://statistics.fibl.org/world/area-world.html?tx_statisticdata_pi1%5Bcontroller%5D=Element2Item&cHash=f367262839ab9ca2e7ac1f333fbb1ca2 (2021).
54. Nowak, B., Nesme, T., David, C. & Pellerin, S. To what extent does organic farming rely on nutrient inflows from conventional farming? *Environ. Res. Lett.* **8**, 044045 (2013).
55. Steffen, W. *et al.* Trajectories of the Earth System in the Anthropocene. *Proc. Natl. Acad. Sci.* **115**, 8252–8259 (2018).
56. Cassman, K. G. & Dobermann, A. Nitrogen and the future of agriculture: 20 years on: This article belongs to Ambio's 50th Anniversary Collection. Theme: Solutions-oriented research. *Ambio* s13280-021-01526-w (2021) doi:10.1007/s13280-021-01526-w.
57. FAO. *FOOD BALANCE SHEETS - A Handbook*. (FAO, 2001).
58. Lassaletta, L. *et al.* Food and feed trade as a driver in the global nitrogen cycle: 50-year trends. *Biogeochemistry* **118**, 225–241 (2014).
59. Smil, V. Crop Residues: Agriculture's Largest Harvest. *BioScience* **49**, 299–308 (1999).
60. Shepon, A., Eshel, G., Noor, E. & Milo, R. Energy and protein feed-to-food conversion efficiencies in the US and potential food security gains from dietary changes. *Environ. Res. Lett.* **11**, 105002 (2016).
61. Lassaletta, L. *et al.* Nitrogen use in the global food system: past trends and future trajectories of agronomic performance, pollution, trade, and dietary demand. *Environ. Res. Lett.* **11**, 095007 (2016).
62. Smil, V. Nitrogen in crop production: An account of global flows. *Glob. Biogeochem. Cycles* **13**, 647–662 (1999).
63. OECD-FAO. *OECD-FAO Agricultural Outlook 2022-2031*. (OECD, 2022). doi:10.1787/f1b0b29c-en.
64. McDuffie, E. E. *et al.* A global anthropogenic emission inventory of atmospheric pollutants from sector- and fuel-specific sources (1970–2017): an application of the Community Emissions Data System (CEDS). *Earth Syst. Sci. Data* **12**, 3413–3442 (2020).
65. Heffer, P., Gruère, A. & Roberts, T. *Assessment of Fertilizer Use by Crop at the Global Level 2014-2014/15*. (International Fertilizer Industry Association, 2017).
66. Einarsson, R. *et al.* Crop production and nitrogen use in European cropland and grassland 1961–2019. *Sci. Data* **8**, 288 (2021).
67. Herridge, D. F., Peoples, M. B. & Boddey, R. M. Global inputs of biological nitrogen fixation in agricultural systems. *Plant Soil* **311**, 1–18 (2008).
68. Berendes, D. M., Yang, P. J., Lai, A., Hu, D. & Brown, J. Estimation of global recoverable human and animal faecal biomass. *Nat. Sustain.* **1**, 679–685 (2018).
69. Ju, X., Gu, B., Wu, Y. & Galloway, J. N. Reducing China's fertilizer use by increasing farm size. *Glob. Environ. Change* **41**, 26–32 (2016).
70. de Vries, W., Kros, J., Kroeze, C. & Seitzinger, S. P. Assessing planetary and regional nitrogen boundaries related to food security and adverse environmental impacts. *Curr. Opin. Environ. Sustain.* **5**, 392–402 (2013).

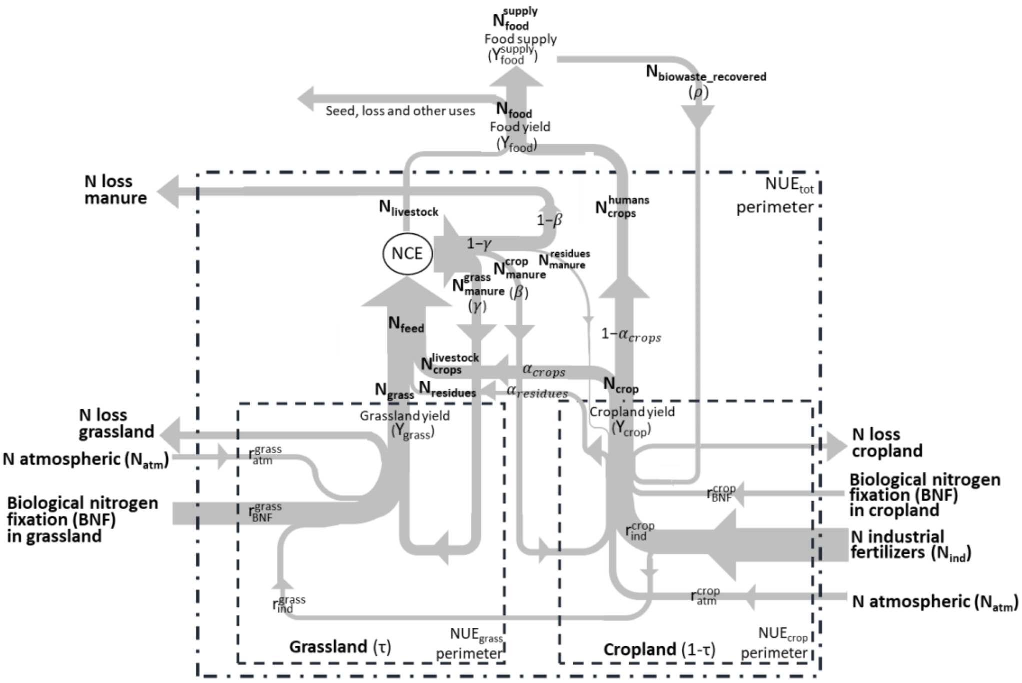

Extended data Figure 1| Flow diagram of the modeling system. Nitrogen (N) flows are indicated in absolute terms (in bold, i.e. kgN·yr^{-1}) and per unit land (in light, i.e. kgN·ha^{-1}·yr^{-1}). τ and (1-τ) are respectively the share of grassland and cropland in total agricultural land. Food production (N_{food}) is total primary production extracted from grassland (N_{grass}) and cropland (N_{crop}), plus crop residues used for feed ($N_{residues}$), plus livestock production ($N_{livestock}$) minus total feed (N_{feed}). N_{food} is human-edible biomass and is the sum of food supply (N_{food}^{supply}), seed, loss and other uses. N_{food} and N_{food}^{supply} per unit agricultural land (ha) are respectively the food yield (Y_{food}) and unitary food supply (Y_{food}^{supply}). α_{crops} and $\alpha_{residues}$ are respectively the shares of N_{crop} and crop residues production used for feed. Total N input (N_{tot} in the equations – not illustrated) is the sum of N input to cropland and grassland from biological nitrogen fixation (BNF), industrial N fertilizers (N_{ind}), atmospheric deposition (N_{atm}) and potential N return to agriculture ($N_{biowaste\_return}$) from human waste management. $N_{biowaste\_return}$ is a fraction (ρ) of N_{food}^{supply}. Total N input divides into N_{food} and N loss. Total system N use efficiency (NUE_{tot}) is the ratio of N_{food} to total N input. NUE_{tot} integrates N use efficiency in cropland (NUE_{crop}) and grassland (NUE_{grass}), livestock proteins conversion efficiency (NCE), the fraction of N excretion voided on grassland (γ) and the share of manure N recovered to cropland (β).

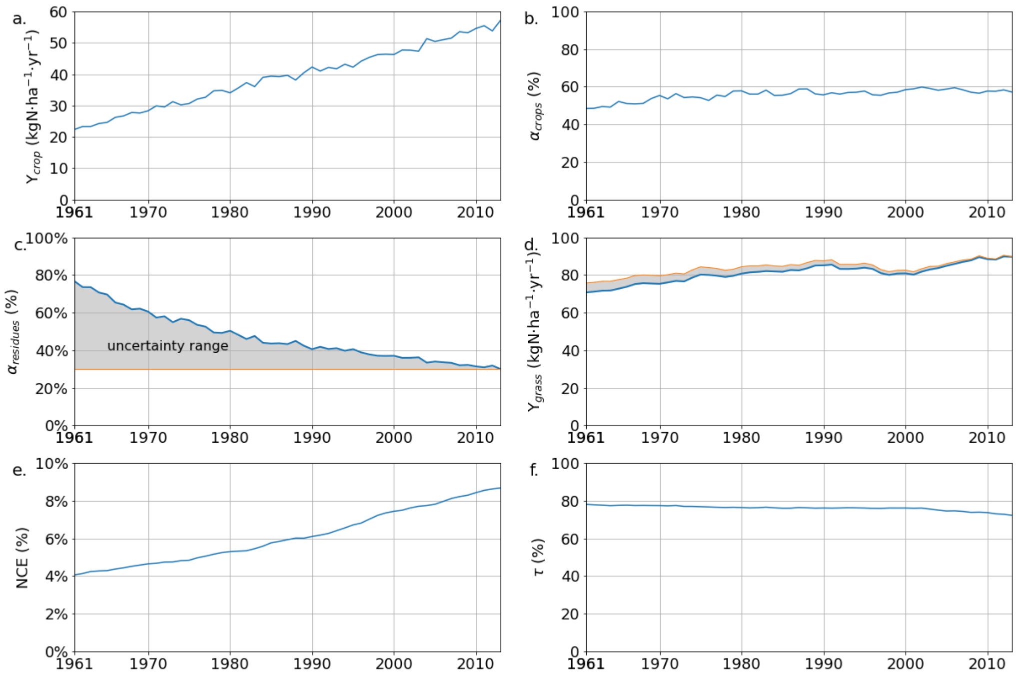

Extended Data Figure 2| Food yield drivers over the benchmark period (1961-2013). Data are from ref. [33]. a. Crop yield (Y_{crop}) b. Share of crops used for feed (α_{crops}). c. Share of crop residues used for feed ($\alpha_{residues}$) including uncertainty between constant share of 30% and decreasing share from 75 to 30% over the period (see Methods) d. Grass yield (Y_{grass}) and uncertainty according to the value of $\alpha_{residues}$ e. Livestock nitrogen conversion efficiency (NCE) f. share of grassland in total agricultural land (τ).

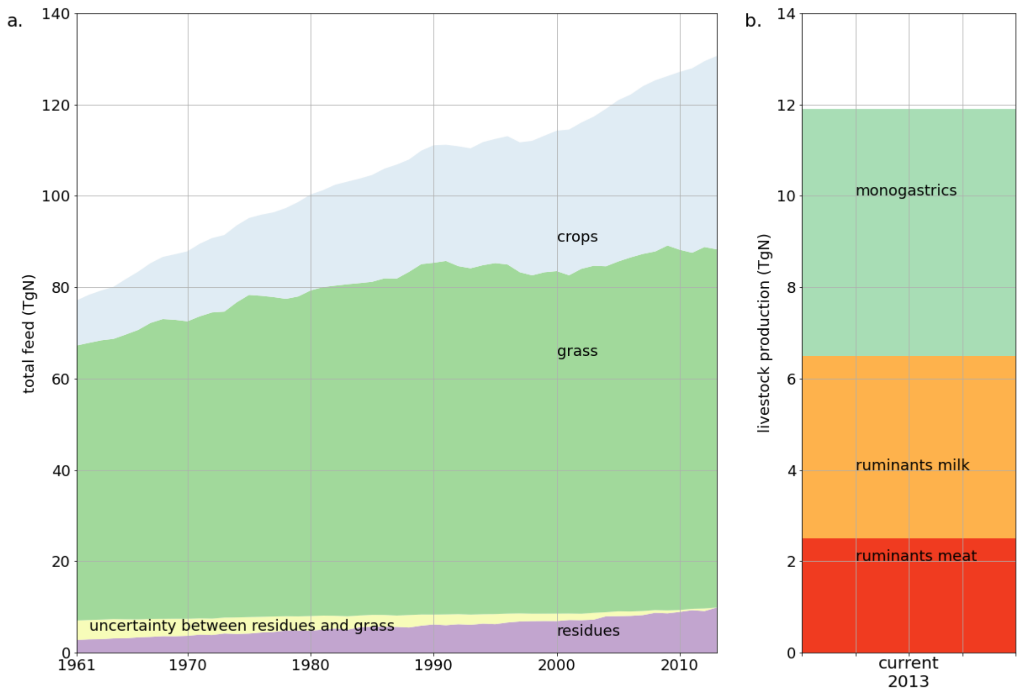

Extended Data Figure 3| a. Total feed (TgN·yr^{-1}) and breakdown among crops, grass and crop residues over the benchmark period (1961-2013) b. Current (2013) total livestock production (TgN·yr^{-1}). Total feed and the amount delivered from crops are derived from FAOSTAT (ref. [33]) as described in Methods. The sum of grass and residues is calculated as the difference between total feed and feed from crops. The relative contribution of grass and crop residues is approximated considering a range for crop residues used for feed from 70 to 30% (see Supplementary Figures 2c,d and Methods). Livestock production is derived from FAOSTAT (ref. [1]) for year 2013 and split into ruminants meat, dairy and monogastric production. Monogastrics are exclusively grain-fed, but feed of ruminants (dairy and beef) also includes crops.

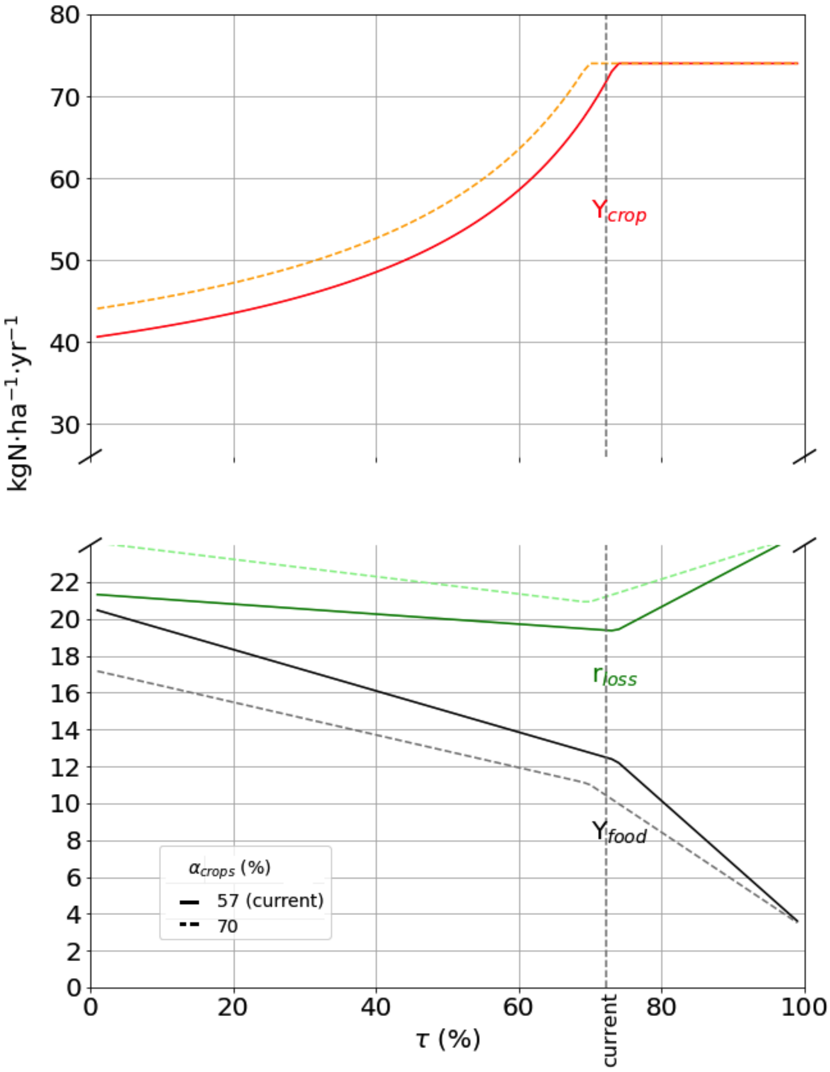

Extended Data Figure 4| Global average crop yield (Y_{crop}), food yield (Y_{food}) and N loss rate (r_{loss}) per unit agricultural land in the organic boundary (B5) in function of the share of grassland in total agricultural land (τ). The calculation is done for biowaste N return to agriculture (ρ) of 30% and for share of crops used for feed (α_{crop}) of 57% and 70%. The vertical dotted line indicates current global τ. The change in slope corresponds to Y_{crop} equaling maximum Y_{crop} (full closure of organic crop yield gap). For Y_{crop} below maximum, Y_{crop} increases with τ (because N limitation per unit cropland decreases with τ), but Y_{food} slightly decreases. For maximum Y_{crop}, the decrease in Y_{food} in function of τ is steeper. The curves highlight that Y_{crop} increases with α_{crops} due to higher manure production, and the increase also depends on the share of manure N return to cropland (β). The higher the β, the faster the increase in Y_{crop} in function of α_{crops}.

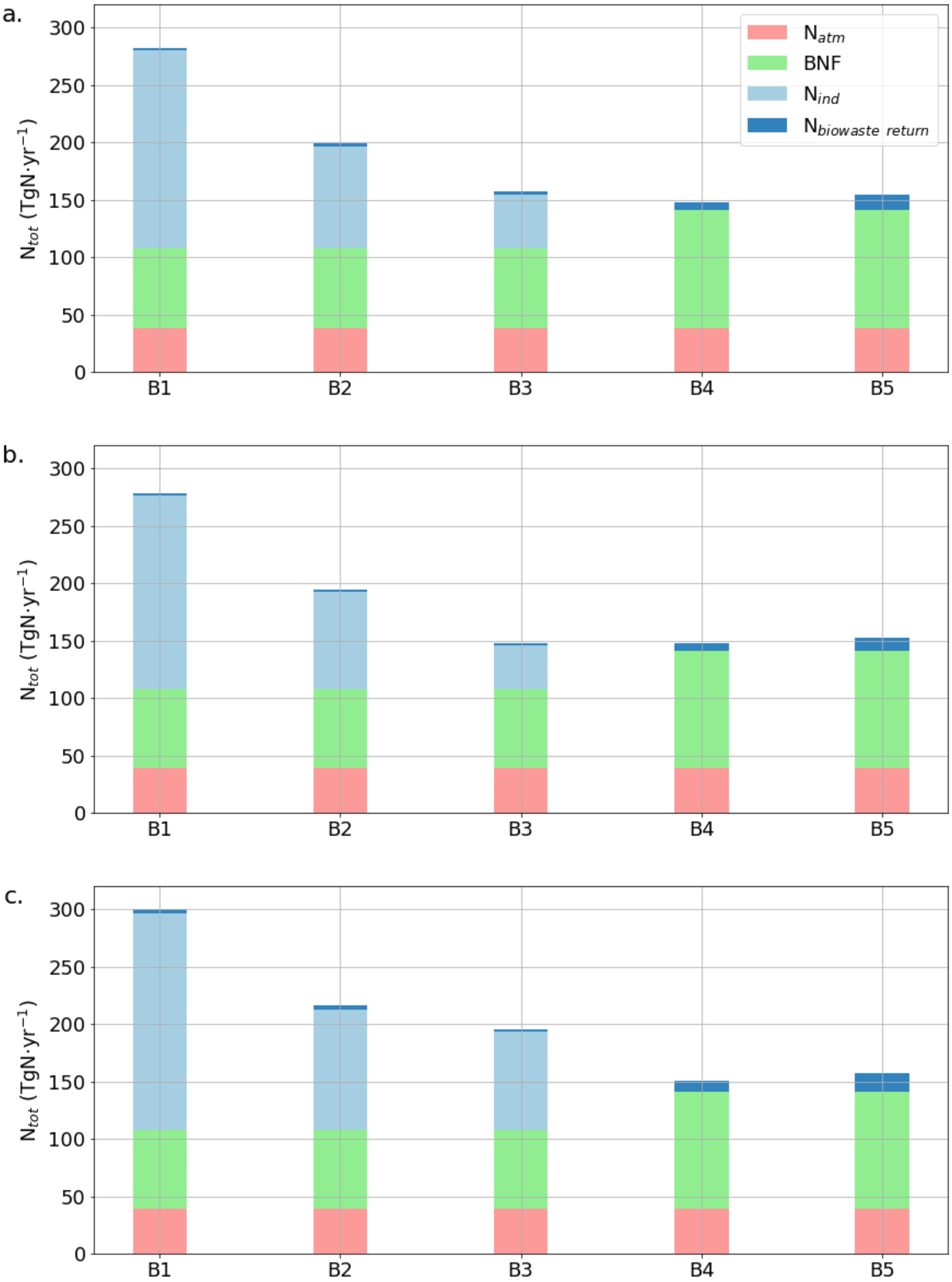

Extended Data Figure 5|Total simulated N input (N_{tot}) per source in the five food production boundaries (B1 to B5). B1-B3 are under industrial fertilization (N_{ind}) and B4-B5 under organic fertilization. N_{tot} is calculated for a. current share of crops used for feed (α_{crops} = 57%) b. α_{crops} = 70% and c. α_{crops} = 0%. N_{tot} is the sum of N input to cropland and grassland. N_{atm} stands for atmospheric N deposition, BNF for biological N fixation, N_{ind} for industrial fertilizers input and $N_{biowaste\_return}$ for biowaste N return to agriculture via human waste management.

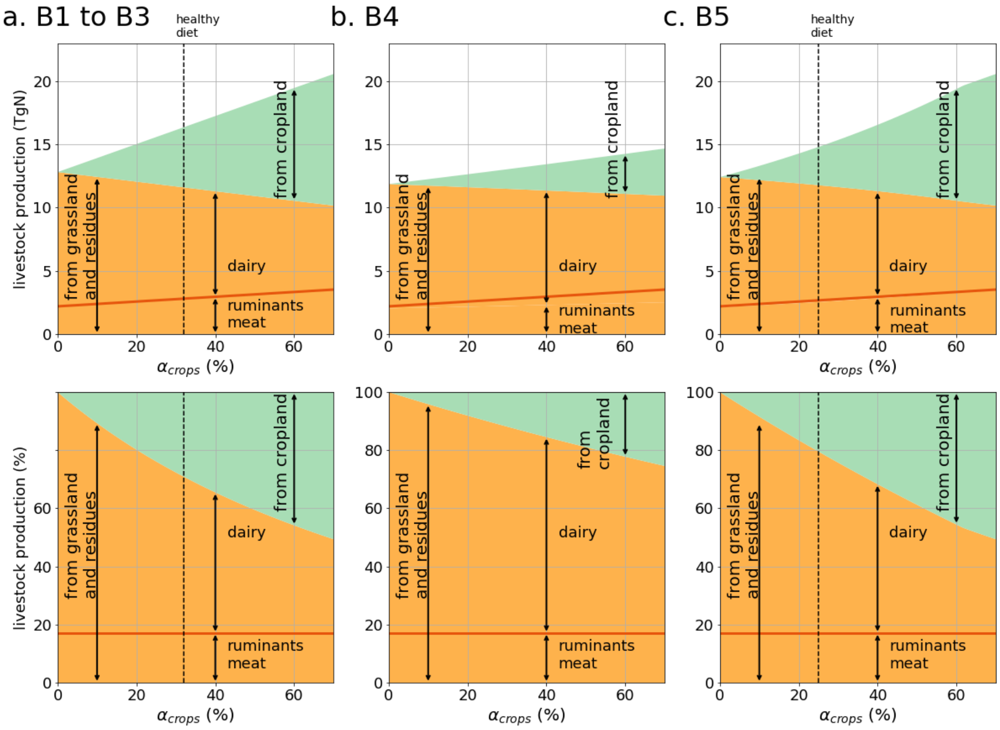

Extended Data Figure 6| Livestock production ($TgN \cdot yr^{-1}$ and %) in global food production boundaries (B1-B5) in function of the share of crops used for feed (α_{crops}). a. Food production boundaries under industrial fertilization (B1-B3). b. Organic food production boundary with current N use efficiency (B4). c. Organic food production boundary with improved N use efficiency (B5)**.** We distinguish between livestock production from grassland and residues (no feed competition) and livestock production from cropland (grain-fed livestock). Production from grassland and residues is dairy and ruminants meat, and production from cropland is undifferentiated between dairy and monogastrics production (pork, poultry and eggs). The red line divides ruminants' production between meat and milk. The vertical dotted lines indicate the share of crops used for feed (α_{crops}) that corresponds to animal proteins content in healthy diet i.e. 26% (ref. [44], Supplementary Table 5). Note that in B4, the share of animal proteins always exceeds the recommendation in healthy diets due to low crop yields.

Extended Data Table 1| Summary table of model variables, abbreviations, and units. Model variables are classified between drivers of food yield, drivers of N cycling, drivers of food yield allocation to food supply, and system-wide variables

Name	Abbreviation	Unit
Drivers of the food yield: 6		
Crop yield	Y_{crop}	kgN·ha^{-1}·yr^{-1} of cropland
Grass yield	Y_{grass}	kg N·ha^{-1}·yr^{-1} of grassland
Livestock nitrogen conversion efficiency	NCE	%
Share of crop residues used for feed	$\alpha_{residues}$	%
Grassland share	τ	%
Share of crops used for feed	α_{crops}	%
Drivers of N cycling: 12		
Atmospheric deposition rate in cropland	r_{atm}^{crop}	kgN·ha^{-1}·yr^{-1}of cropland
Atmospheric deposition rate in grassland	r_{atm}^{grass}	kgN·ha^{-1}·yr^{-1}of grassland
Biological N fixation rate in cropland	r_{BNF}^{crop}	kgN·ha^{-1}·yr^{-1}of cropland
Biological N fixation rate in grassland	r_{BNF}^{grass}	kgN·ha^{-1}·yr^{-1}of grassland
N industrial rate in cropland	r_{ind}^{crop}	kgN·ha^{-1}·yr^{-1} of cropland
N industrial rate in grassland	r_{ind}^{grass}	kgN·ha^{-1}·yr^{-1}of grassland
N use efficiency in cropland	NUE_{crop}	%
N use efficiency in grassland	NUE_{grass}	%
Nitrogen harvest index of crops	NHI	%
Fraction of N voided on grassland	γ	%
Share of manure N recovered to cropland	β	%
Biowaste N return to agriculture	ρ	%
Drivers of food yield allocation to food supply: 4		
Vegetal proteins	$\delta_{vegetal}$	%
Animal proteins	δ_{animal}	%
Weighted average vegetal/animal proteins	$\delta_{weighted}$	%
Annual food supply per capita	n_{food}^{supply}	kgN·cap^{-1}·yr^{-1}
System-wide variables: 6		
Food yield	Y_{food}	kgN·ha^{-1}·yr^{-1} of total agricultural area
Total agricultural land	AL	ha
Feeding capacity	Global_pop	inhabitants
Share of animal proteins in food supply	$Share_{animal}$	%
N loss rate	r_{loss}	kgN·ha^{-1}·yr^{-1} of total agricultural area
Total N use efficiency	NUE_{tot}	%
Sum of model variables: 28		

Extended Data Table 2 | Summary table of model variables classified between input and output over the benchmark period and global weighted average data in 1961 and 2013. Model input variables are further distinguished between constant and fluctuating. Model output variables are systematically validated with literature data whenever available.

Model variables		Global weighted average values	
Abbreviation	unit	1961	Current (2013)
Constant model input variables: 3			
NHI	%	70	70
γ	%	50	50
NUE_{grass}	%	75	75
Fluctuating model input variables: 18			
Y_{crop}	$kgN{\cdot}ha^{-1}{\cdot}yr^{-1}$	22.3	57.0
Y_{grass}	$kgN{\cdot}ha^{-1}{\cdot}yr^{-1}$	17.6	22.0
$\alpha_{residues}$	%	78	30
τ	%	78.1	72.2
α_{crop}	%	48	57
r_{atm}^{crop}	$kgN{\cdot}ha^{-1}{\cdot}yr^{-1}$	5	8
r_{atm}^{grass}	$kgN{\cdot}ha^{-1}{\cdot}yr^{-1}$	5	8
r_{BNF}^{crop}	$kgN{\cdot}ha^{-1}{\cdot}yr^{-1}$	10.9	24.8
r_{ind}^{crop}	$kgN{\cdot}ha^{-1}{\cdot}yr^{-1}$	11.6	76.1
r_{ind}^{grass}	$kgN{\cdot}ha^{-1}{\cdot}yr^{-1}$	0.15	1.50
NCE	%	4.1	8.6
ρ	%	30	5
$\delta_{vegetal}$	%	69	63
δ_{animal}	%	97	99
$\delta_{weighted}$	%	75	72
β	%	47.7	35.4
AL	ha	4.36×10^9	4.84×10^9
n_{food}^{supply}	$kgN{\cdot}cap^{-1}{\cdot}yr^{-1}$	3.43	4.43
Model validation output variables: 4			
Y_{food}	$kgN{\cdot}ha^{-1}{\cdot}yr^{-1}$	3.25	9.15
$Share_{animal}$	%	29	35
NUE_{crop}	%	44.6	44.0
Global_pop	inhabitants	3.09×10^9	7.22×10^9
Model output variables (for which no reference data exist): 3			
r_{BNF}^{grass}	$kgN{\cdot}ha^{-1}{\cdot}yr^{-1}$	9.93	10.24
r_{loss}	$kgN{\cdot}ha^{-1}{\cdot}yr^{-1}$	15.1	35.6
NUE_{tot}	%	17.5	20.5
Sum of model variables: 28			

Extended Data Table 3 | Summary table of model variables classified between input and output in the five global food production boundaries (B1-B5), and data used in the simulations. Model input variables are further distinguished between constant and affected with a range. a. Global food production boundaries under industrial fertilization (B1, B2, B3). b. Global food production boundaries under organic fertilization (B4, B5). Values in square brackets indicate minimum-maximum range for model input variables in a given boundary.

a.

Model variables		Global food production boundaries under industrial fertilization		
Abbreviation	unit	B1	B2	B3
Constant model input variables: 17				
Y_{crop}	kgN·ha^{-1}·yr^{-1}	74	74	74
Y_{grass}	kgN·ha^{-1}·yr-1	29	29	29
NCE	%	11.2	11.2	11.2
$\alpha_{residues}$	%	30	30	30
r_{atm}^{crop}	kgN·ha^{-1}·yr^{-1}	8	8	8
r_{atm}^{grass}	kgN·ha^{-1}·yr^{-1}	8	8	8
r_{BNF}^{crop}	kgN·ha^{-1}·yr^{-1}	24.8	24.8	24.8
r_{BNF}^{grass}	kgN·ha^{-1}·yr^{-1}	10.2	10.2	10.2
NUE_{grass}	%	75	75	75
γ	%	50	50	50
ρ	%	5	5	5
NHI	%	70	70	70
AL	ha	4.84×10^{9}	4.84×10^{9}	4.84×10^{9}
δ_{animal}	%	100	100	100
$\delta_{vegetal}$	%	69	69	69
$\delta_{weighted}$	%	72	72	72
n_{food}^{supply}	kgN·cap^{-1}·yr^{-1}	4.43	4.43	4.43
Model input variables with range: 4				
α_{crop}	%	[0, 70]	[0, 70]	[0, 70]
τ	%	[70.2, 72.3]	[70.2, 72.3]	[70.2, 72.3]
NUE_{crop}	%	44.3	70	70
β	%	35.4	35.4	80
Model output variables: 7				
Y_{food}	kgN·ha^{-1}·yr^{-1}	output	output	output
$Share_{animal}$	%	output	output	output
Global_pop	inhabitants	output	output	output
r_{ind}^{crop}	kgN·ha^{-1}·yr^{-1}	output	output	output
r_{ind}^{grass}	kgN·ha^{-1}·yr^{-1}	output	output	output
r_{loss}	kgN·ha^{-1}·yr^{-1}	output	output	output
NUE_{tot}	%	output	output	output
Sum of model variables: 28				

b.

Model variables		Global food production boundary under organic fertilization	
Abbreviation	unit	B4	B5
Constant model input variables: 14			
NCE	%	11.2	11.2
$\alpha_{residiues}$	%	30	30
r_{atm}^{crop}	kgN·ha^{-1}·yr^{-1}	8	8
r_{atm}^{grass}	kgN·ha^{-1}·yr^{-1}	8	8
r_{ind}^{crop}	kgN·ha^{-1}·yr^{-1}	0	0
r_{ind}^{grass}	kgN·ha^{-1}·yr^{-1}	0	0
NUE_{grass}	%	75	75
γ	%	50	50
NHI	%	70	70
AL	ha	4.84×10^{9}	4.84×10^{9}
δ_{animal}	%	100	100
$\delta_{vegetal}$	%	69	69
$\delta_{weighted}$	%	72	72
n_{food}^{supply}	kgN·cap^{-1}·yr^{-1}	4.43	4.43
Model input variables with range: 7			
α_{crop}	%	[0, 70]	[0, 70]
τ	%	[70.2, 72.3]	[70.2, 72.3]
NUE_{crop}	%	44	70
β	%	35.4	80
ρ	%	[5,30]	[5,30]
r_{BNF}^{crop}	kgN·ha^{-1}·yr^{-1}	[24.8, 30]	[24.8, 30]
r_{BNF}^{grass}	kgN·ha^{-1}·yr^{-1}	[10.2, 18]	[10.2, 18]
Model output variables: 7			
Y_{crop}	kgN·ha^{-1}·yr^{-1}	output	output
Y_{grass}	kgN·ha^{-1}·yr^{-1}	output	output
Y_{food}	kgN·ha^{-1}·yr^{-1}	output	output
$Share_{animal}$	%	output	output
Global_pop	Inhabitants	output	output
r_{loss}	kgN·ha^{-1}·yr^{-1}	output	output
NUE_{tot}	%	output	output
Sum of model variables: 28			